Optical Biosensors

First Semester Report
Fall Semester 2007

by
Allan Fierro
David Sehrt
Doug Trujillo
Evan Vlcek
Michael Bretz

Prepared to partially fulfill the requirements for
ECE401

Department of Electrical and Computer Engineering
Colorado State University
Fort Collins, Colorado 80523

Report Approved: _____

Project Advisor

_____

Senior Design Coordinator

ABSTRACT

Currently, in order to sort and scan cells quickly and efficiently one has to use flow cytometry or some related process. One of the major components of flow cytometry is the use of labels, fluorescent dyes and markers, in order to tell cells or cell parts apart from other cells or cell parts. Fluorescent dyes are expensive and light sensitive, so care has to be used in working with them, and samples to be tagged must be kept in the dark. Also, there must be a large number of cells in order to run flow, and depending on the situation that may be very difficult. After flow cytometry the samples are contaminated or dead. Plus, the machine is very expensive with the initial cost and upkeep maintenance, so that signing up for flow time is quite expensive. Then there is the training that is needed to operate the flow cytometer. All of these factors add to the time and trouble needed to analyze the cell samples by flow cytometry. If a way can be found to do cell analysis without needing to fluorescently tag the samples, the process of analysis would be cheaper and quicker, both of which are very desirable traits.

We have attempted to design a system that uses the reflective index of the cells, by measuring the difference in the light detected in the cells of interest, rather than using a fluorescent dye. This technique will solve many of the problems associated with traditional flow cytometry. Our technique will save us from having to fluorescent tag our samples and we will be able to retrieve our cell samples alive after the trapping and analyzing of them, something which cannot be done with current flow cytometry techniques. We will not need as many cells in our sample as well, plus this should reduce the cost of upkeep and operation.

The components of our system are the microscope, the cell detection circuit, the analog to digital convertor and computer control software and the chip with the channel on it. To date, we have made a channel to flow our sample solution through. This channel has metal leads for setting up the electric field to trap our cell when it is detected by the detection circuit to be analyzed by the spectrometer. We first had to build the channels with the traps on them. The next step was to determine the proper flow rate of the solution so as to optimize trapping. We also made a circuit to detect the presence of a cell to trigger the trap. All of the control was done with Labview software.

TABLE OF CONTENTS

FIGURES

Chapter I: Introduction

Flow cytometry is a technique for counting, examining, and sorting microscopic particles suspended in a stream of fluid that has been around since the mid 1970s. It allows simultaneous multiparametric analysis of the physical and/or chemical characteristics of single cells flowing through an optical and/or electronic detection apparatus. A beam of light (usually laser light) of a single wavelength is directed onto a hydro-dynamically focused stream of fluid. A number of detectors are aimed at the point where the stream passes through the light beam; one in line with the light beam (Forward Scatter or FSC) and several perpendicular to it (Side Scatter (SSC) and one or more fluorescent detectors). Each suspended particle passing through the beam scatters the light in some way, and fluorescent chemicals found in the particle or attached to the particle may be excited into emitting light at a lower frequency than the light source. This combination of scattered and fluorescent light is picked up by the detectors, and by analyzing fluctuations in brightness at each detector (one for each fluorescent emission peak) it is then possible to extrapolate various types of information about the physical and chemical structure of each individual particle. FSC correlates with the cell volume and SSC depends on the inner complexity of the particle, for example, the shape of the nucleus, the amount and type of cytoplasmic granules or the membrane roughness. Flow cytometers form images of each cell's fluorescence, scattered light, and transmitted light. Modern flow cytometers are able to analyze several thousand particles every second, in "real time", and can actively separate and isolate particles having specified properties. A flow cytometer is similar to a microscope, except that instead of producing an image of the cell, flow cytometry offers "high-throughput" (for a large number of cells) automated quantification of set parameters. To analyze solid tissues single-cell suspension must first be prepared. Fluorescence-activated cell sorting (FACS) is a specialized type of flow cytometry. It provides a method for sorting a heterogeneous mixture of biological cells into two or more containers, one cell at a time, based upon the specific light scattering and fluorescent characteristics of each cell. It is a useful scientific instrument as it provides fast, objective and quantitative recording of fluorescent signals from individual cells as well as physical separation of cells of particular interest.

The term optofluidics defines an emergent research field that combines microfluidics and optics and from this a class of adaptive optical circuits that integrate optical and fluidic devices. In many biological applications the two technologies are used in combination-microfluidics for sample delivery and optics for sensing. The introduction of liquids in the optical structure enables flexible fine-tuning and even reconfiguration of circuits such that they may perform tasks optimally in a changing environment. The use of fluid as a medium for transport is appropriate for a significant class of clinically important biological entities, ranging from DNA strands, viruses, and bacteria to cells and microorganisms. In addition, microfluidics-based devices require very low input sample volumes (nanoliters or less) and can be very conservative in terms of the samples. The implementation of optics in the microfluidic platform enables an unprecedented level of integration. Moreover, optofluidic devices are easily and highly

reconfigurable, which can be a significant advantage for manipulating and handling biological samples.

The goal of our project is to design a system of cell detection and analyses without the need for fluorescent markers or tags. This will help reduce the cost as well as the time involved in sample preparation. Another benefit of such a system is the ability to keep the samples for further use, all of which cannot be done with tradition flow cytometry. If we are successful there is a large market for our product, mostly in the biological fields.

Chapter two will discuss the fabrication of our chips and how the channels are made and how the traps and leads are added to the chip. Chapter three will be on DEP chip micro-fluidic ports. Chapter four will discuss the flow control of the microfludics we used plus the pump system. Chapter five will discuss the detection circuit we designed and some of the components used. Chapter six will discuss DEP trapping. Chapter seven will cover the future work and what we plan to do next semester.

Chapter II: Channel Fabrication

Photolithography was used to fabricate these Dielectrophoreris Traps in the CSU Cleanroom. This process allows building contacts, wires, and effectively traps on a micron scale. The DEP chips were built with two distinct components, a DEP trapping circuit and a microfluidic channel. These two components are bonded together to form a DEP trap.

The DEP trapping circuit is composed of three contacts and three discrete lines running through the area under the channel. The conductive material used was gold and chrome. These metals were first deposited onto a glass slide using an Evaporator in the cleanroom. A layer 30nm of chrome was first deposited onto the slide. This thin layer of chrome is deposited because chrome can adhere to glass much better than gold can. A 120nm layer of gold is then placed over the chrome layer. Gold is deposited because of its low resistance. Once this deposition is completed, photolithography follows. AZ1512 Photoresist is placed and then spun on the chip. This resist is thinner and has very good resolution. A soft bake at 110 degrees Celsius for 1 minute follows. Next the chrome DEP mask is used to pattern the resist. A chrome mask is chosen for this exposure because of the small features it encompasses. Chrome masks are expensive but have a high resolution and have an antireflective coating to enhance the exposure. This mask contains two different trapping circuits to select from. A characterization of the AZ1512 resist found and exposure time with the soft bake of 10 seconds. The resist is exposed for 10 seconds which maximizes the resolution of the resist. The exposed resist is then developed leaving the unexposed area covered. A two step wet etch removes the uncovered gold and
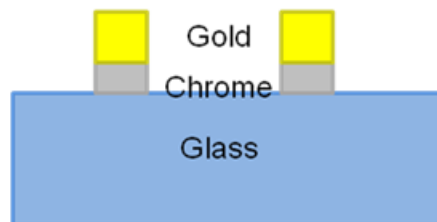

Figure 2.1

chrome from the glass slide. The DEP trap chip is then ready for two of the three types of bonding. The DEP channels were composed of either polydimethylsiloxane (PDMS) or glass. PDMS channels were the majority of the channels prepared since the fabrication success rate of these channels were much higher than glass. The success of PDMS is attributed to its exceptional adherence to glass. The PDMS used was made of bulk PDMS and the PDMS curing agent with a mass ratio of 10:1 respectively. This PDMS is then placed in a vacuum and degassed. Degassing will remove the impurities in the PDMS which will improve the optical properties of the mold. A mold of the channel was needed to form the channel. This mold composed of a silicon substrate and SU-8 resist. This resist is much thicker and viscous than the AZ1512 and can be used as a mold when it is baked and fully developed. Once the mold is constructed PDMS is poured into the mold again degassed. Once degassed the mold is placed in an oven to bake for at least 4 hours. The curing agent transforms this viscous liquid into an elastic solid. The PDMS can then be cut and peeled off the silicon substrate. A glass cover slip is then placed on the opposite side of the channel which keeps the PDMS chip clean and allows the channel to be transported easier. In order for the PDMS channel to be bonded to the DEP trapping circuit one more step in the DEP circuit must be performed. A gold and chrome sheet still remains outside of the trapping circuit which is used for other bonding processes. This area is removed with the same lithography steps as creating the traps except that a mask covering the trapping circuit is used. Now the two chips are ready to be bonded together. The DEP chip is taped to a glass slide with the circuit facing out. Both chips are then oxygen-plasma treated with a micro-RIE. After treatment the two chips are bonded together using the mask aligner. The PDMS channel is placed on the stage facing up. The DEP chip is positioned facing down being held in the mask holder. The DEP traps are then positioned over the channel. The channel is then brought into contact with the DEP circuit chip. The two are now bonded together. The mask holder is then unscrewed and pulled out vertically from the aligner.

Glass channels were experimented with as well. These glass channels are more desirable than PDMS because a dielectric coating can be deposited on the surface of glass producing a light modulating cavity necessary for cell differentiation. Pyrex glass is used for channel etching and chrome and gold are deposited on the surface. A thick layer of P4400 positive resist is deposited onto the surface. This resist was chosen because it is much thicker than the AZ1512 resist which will be necessary with HF etching. The tradeoff with using P4400 is that it doesn't have as good a resolution as AZ1512. In this application giving up resolution is certainly acceptable. The soft bake for this resist is 110 degrees Celsius for 2 minutes. The resist is then exposed with the channel mask for 35 seconds. The exposed area is washed away in development. The chip is then baked at 110 degrees Celsius for 10 minutes. This turns the resist into a hard film which can withstand the wet etching process. The gold and chrome are etched away. The next step is to etch the glass. This is done using a wet etch of HF. The chip is placed in HF for approximately 3-4 minutes. The chip is removed from the HF and washed with deionized water. The chip is then placed in an acetone bath to remove the hardened resist. Acceptable glass etching was never achieved in the semester. The channel surface must be as

uniform as possible to provide better transmission of light. Using an alpha step to measure the surface height, deep indents were found in the glass. One explanation to this result is that there are lattice impurities in the glass that etch faster than the uniform lattice. If this were the case then higher quality glass would be needed to perform suitable glass etching.

Once the layer of resist is removed, the channel chip can be bonded to the DEP trapping circuit chip. Two bonding methods have been implemented. The more successful method is Indium bonding. A piece of Indium metal and the channel with gold on the outer area are placed in a solution. A positive voltage is applied to the Indium metal and a negative voltage is place on the of the channel chip. This creates a current of Indium to be deposited on the gold. The channel chip is then ready to bond to the DEP circuit chip. The two pieces are roughly aligned by eye and pressed together by hand. The chips are then observed under a microscope to view the alignment. Fine adjustments are made to optimize the alignment. Once the alignment is made the two chips are sandwiched between two copper sheets. These sheets are then put in a vice. The vice is screwed together with four screws. This puts equal pressure on the bonding area. The bonding vice is then placed into a heater. A vacuum is pulled in the heater to prevent oxidation from the high temperatures. The temperature in the heater is controlled by a programmable unit attached to the heater. The temperature is then programmed to ramp up to and hold at a certain temperature and then ramp down. Once the desire temperature program completes, the bonding vice is pulled from the heater. The channel and the DEP trapping circuit chips are now bonded together.

Figure 2.2
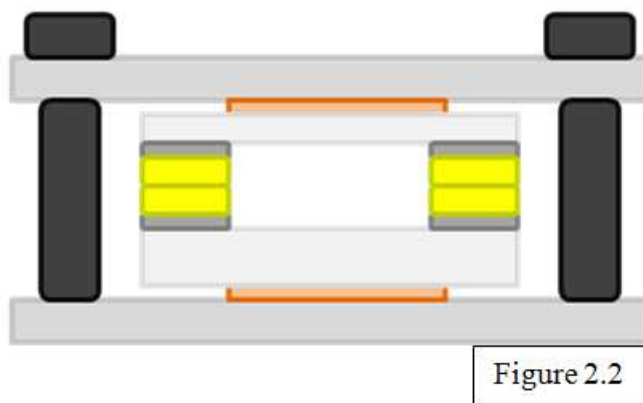
A similar bonding procedure is gold to gold bonding. The advantage gold has over Indium is that the height of the material required for bonding is minimal compared to Indium. Minimizing the height for bonding is critical because the height dictates how leaky the channel will become. Indium bonding adds another layer in the bonding area outside of the chip. This layer adds an additional height on the scale of microns. This will produce a leakier channel than chips bonded with a gold to gold method. This method has not successfully been completed on test chips. These test chips are half the size of the DEP trapping circuit chips and have gold with no patterning. The two gold chips are pressed together and put between the copper plates and into the vice. The temperature is programmed to be much higher than indium bonding. This is due to the fact that Indium bonds much easier to surfaces than gold does to gold or any other surface. The melting point of gold is also very high. In order to fuse the two pieces together a very high temperature must be obtained. An appropriate temperature and pressure have no been

obtained which prevent acceptable bonding. Small bonding areas have been obtained but not large enough to be a reliable method for chip bonding.

Chapter III: DEP Chip Micro-Fluidic Ports

In order to get cells into the DEP chip with a micro-channel, there must be a way for cells to physically enter the chip. It is also important that there is a way for the cells to exit the chip. This is accomplished through the use of nanoports. There are two nanoports on every chip, one for the cells to enter into the channel, and one for cells to exit the channel. Nanoports are cylindrical shaped parts that on the order of 1 – 2 cm in diameter and 2 – 3 cm tall. They are composed of a plastic-like material. On the bottom of the nanoports, there is a small circular opening with a rubber seal surrounding it. From the top, nanoports are hollow with threads so that a nanotube can be secured into the nanoport using a hollow screw-like adapter. These adapters are included as a kit when nanoports are purchased. Nanotubes are very small tubing that are 150 µm in diameter that are frequently used in micro-fluidics. The figure below shows the basic structure of a nanoport.
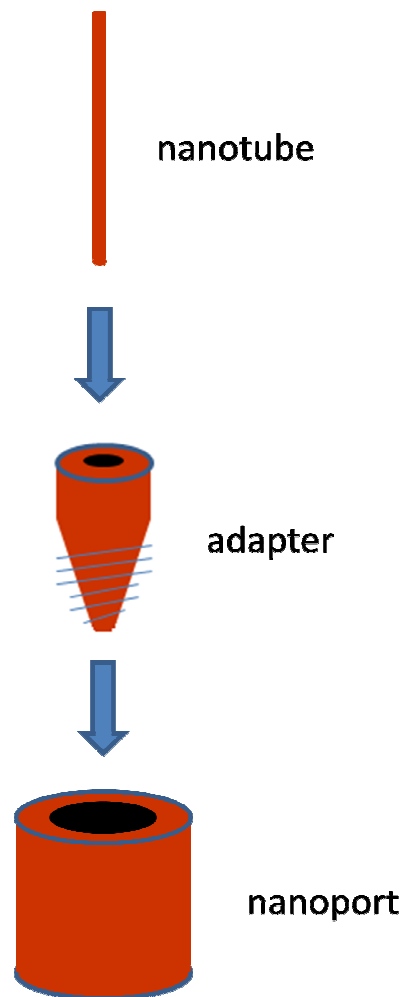
nanotube

adapter

nanoport

Figure 3.1

Before nanoports can be placed on a chip, holes must be drilled into the chip in the appropriate places. To do this, a pattern of the chip fabrication is placed over the chip and the two places for holes are marked. Then a drill press is used with a small drill bit. Great care must be taken when drilling the holes because glass cracks and chips very easily. Water is applied at the drill area and only very small depths are drilled at a time. This process is very dependent on minimal human error. Many of the fabricated chips have non-ideal holes when drilling is complete.

It is also very important to have a way to securely place the nanoports on the DEP chip so that there is no leakage as cells and liquids are pushed into the channel and pulled back out of the channel. This process is quite simple. Adhesive o rings are used to create the bond between the nanoport and the chip. Adhesive o rings are a sticky, glue-like material in an "O" shape that act as double-sided tape. These rings are very carefully placed around the center of the drilled holes, and pressed firmly into place. After this, the nanoports are cautiously placed on the adhesive o rings, making sure to center the nanoport over the hole. Again, this is pressed firmly into place. Once complete, the chip is clamped to the nanoport for one hour to allow the adhensive o ring to dry and seal. The figure below shows the placement of a nanoport.
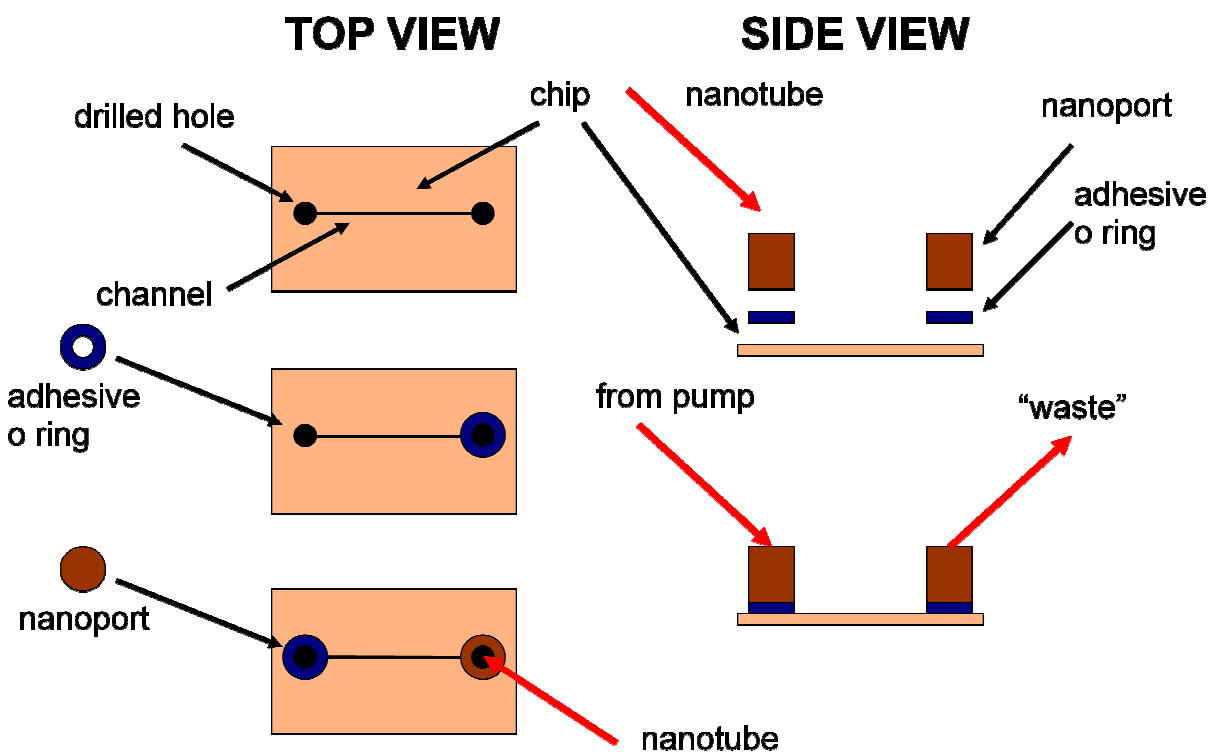

Figure 3.2

Chapter IV: Flow Control

An essential part of the project is to be able to get cells into the chip. There are several considerations for acceptable means to accomplish the desired flow rate of cells in the channel of the chip. The first and primary requirement is that the flow rate must be less than or equal to 40 µm per second (40 µm/s). This requirement comes from the DEP traps on the chip. If the flow rate exceeds 40 µm/s the force of the DEP trap to stop a cell will not be sufficient to stop a cell and hold it in place. Another limitation of flow control is that there must not be too much pressure on the nanoport-chip seal or in the channel. The bonding on glass to glass chips is not very strong and high micro-fluidic pressure will cause the chip to leak. If leaking is severe, it is possible for cells to flow outside of the channel. Obviously, this is very undesirable because all of the traps and optical detection are near the center of the channel. It is also worth noting that all of the glass chips have gaps between the two pieces of glass due to an imperfect bonding process. This creates flow outside of the channel and different fluid dynamics than the PDMS chips. Because the glass to glass chips (glass chips) essentially have larger channels, the flow rate is significantly slower than in the PDMS chips when the same amount of pressure is applied to the fluid.

Most cell samples, such as blood, are obtained using a syringe. Therefore, a syringe is used to push samples into a nanotube and into the channel. Although the end goal of the project is to pump cells through the channel and analyze them, it is impractical to actually use cell samples to develop and test flow control. Therefore, de-ionized water was used with glass spheres ranging from 5 µm to 26 µm in diameter. The majority of the time 9.77 µm spheres were used. This water with glass spheres will be referred to as "fluid" in parts of this section. When the project first began, it was thought that the rate at which the end of a syringe plunger needed to be pushed could be calculated based on the fact that the volume in is the same as the volume out. Ideally, chips are fabricated with a 200 µm wide by 25 µm deep channel. This gives an ideal cross-sectional area of 200 µm × 25 µm = 5000 µm^2. If the syringe plunger is pushed at a rate of x µm/s then the volume of fluid flowing into the nanotube (and the chip) is $\pi \times (0.5 \times$ diameter of syringe [µm]$)^2 \times$ x µm/s = z µm^3/s. This flow rate must logically be the same in the channel since the volume in must equal the volume out. This result can then be used to calculate the velocity at which fluid will travel through the channel. The equation is as follows: v µm/s = z µm^3/s × (5000 µm^2)$^{-1}$. Substituting the first equation into the second gives a direct relationship between the velocity of fluid in the channel v [µm/s] and the velocity at which the plunger of the syringe is pushed x [µm/s]. This resulting equation is:

$$\textbf{v µm/s = x µm/s} \times \boldsymbol{\pi} \times \textbf{(0.5} \times \textbf{diameter of syringe [µm])}^2 \times \textbf{(5000 µm}^2\textbf{)}^{-1}$$

The only syringes on hand at the beginning of the project were 3 cc syringes with a diameter of 8.585 mm = 0.008585 µm manufactured by B-D. Using the equation above equation, to achieve a 40 µm/s flow rate in the channel, the plunger must be pushed at a rate of 0.00346 µm/s. The original plan for flow control was an industrial syringe pump. Borrowed from the chemistry department, the NE – 1000 syringe pump made by New Era Pump Systems, Inc. can push this B-D syringe at a rate of 2.434 µL/hr. This is the equivalent of 6.761×10^5 µm/s. This is 1.954×10^8 times too fast! Obviously this syringe pump is not a valid solution to the flow rate problem. In addition, when the syringe pump was set to its slowest

setting, the torque broke the encoder coupler because the pressure in the chip created a force pushing back against the syringe plunger that was beyond what the pump was designed for.

As a solution, the Oriel Instruments Encoder Mike Controller 18011 was chosen to function as a custom pump. The Oriel Instruments Encoder Mike Controller 18011 (Oriel) is designed to be used as a precise way to move a microscope stage. It can move the actuator at a minimum velocity of 0.5 µm, which is still about 150 times faster than the desired rate for the larger syringe (8.585 mm diameter). To reduce the rate at which the plunger must move, a smaller syringe (4.669 mm diameter) was chosen to be used in the system. This syringe plunger only needs to move at a rate of 0.0115 µm/s to achieve the desired flow rate of 40 µm/s in the channel. Because this is still slower than what the Oriel is capable of, Labview software was used to create a duty cycle where the actuator is only moving for a small percentage of the time. For details on how the Oriel was implemented into the system, see Appendix C2. To achieve 40 µm/s velocity inside the channel, the Labview VI was set so that the actuator moved for 0.825 seconds at 0.5 µm/s (0.4125 µm) and off for 7 seconds. When the VI is used, the optimal flow rate occurs at this duty cycle of approximately 10.5%. This "duty cycle" description applies to the movement of the actuator. However, "duty cycle" is not an accurate comparison because the flow rate in the channel takes much longer to decay than the 7 second period during which the pump is turned off. This is discussed more later. Another consideration is that the stage mounted to the actuator is spring-loaded and adds complication to the analysis. This spring action actually allows the plunger to be pushed at a rate slower than the 0.5 µm/s that the actuator is moving.
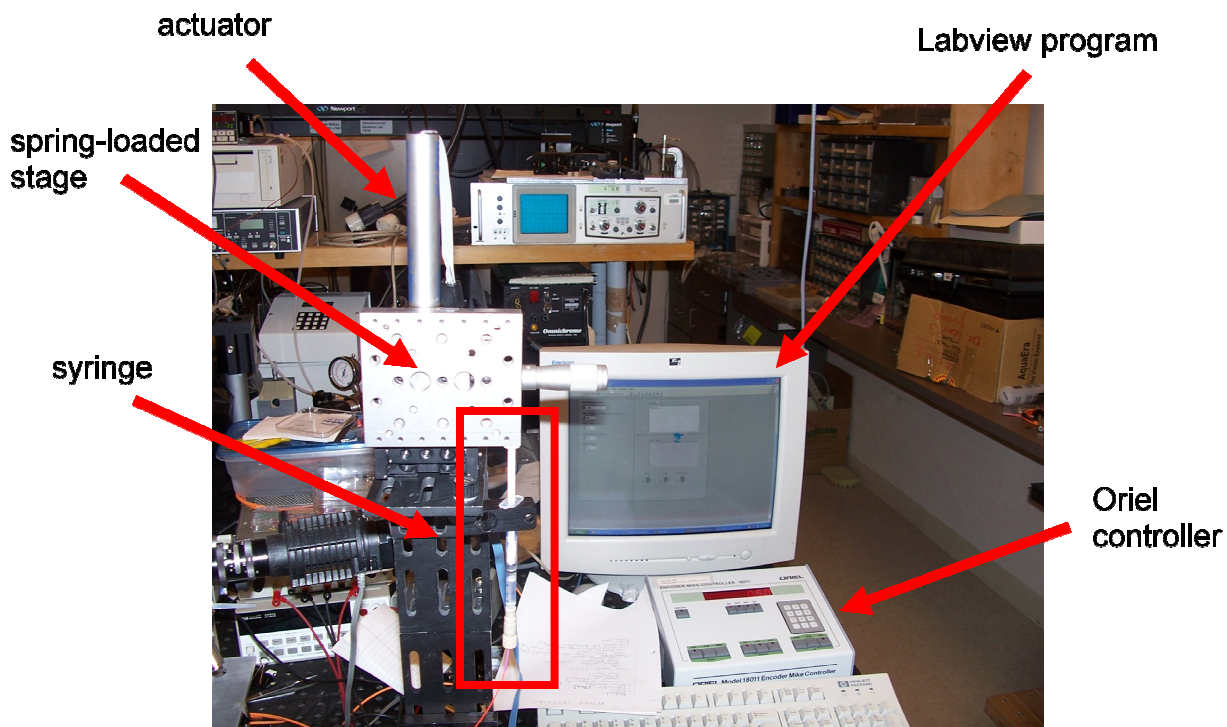

Figure 4

Through experimentation, it was quickly discovered that the derived equation does not hold true for glass chips, but is reasonable for PDMS chips. This is because the actual cross-section in a glass chip's channel is larger and cannot be accurately estimated. Experimentation also revealed that due to complex pressure dynamics, the flow rate in the channel does not follow the syringe plunger. To be more precise, when the plunger is moved and then stopped, the flow in the channel does not stop immediately, but rather decays over the course of several minutes. This behavior is analogous to the behavior to an RC circuit. Both have a time constant associated with how long it takes the flow rate to die down. The larger syringe (8.585 mm diameter) builds up a higher pressure and the time constant is several times longer than the time constant for the smaller syringe (4.699 mm diameter). This suggests that the cross-sectional area of the syringe is proportional to the time constant for the flow rate inside the channel. All of these more complex dynamics make experimentation the best indication of actual flow inside the channel. There was no precise way to obtain the velocity of spheres moving in the channel, but the duty cycle described earlier is estimated to produce a flow rate of 40 µm/s in a PDMS channel. Due to limited fabrication of glass chips near the end of the semester, the duty cycle for the desired flow rate in a glass chip has not been found. However, it is known that the duty cycle must be higher than that for the PDMS channel.
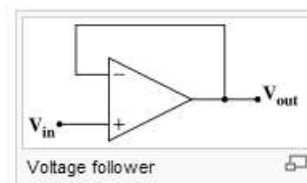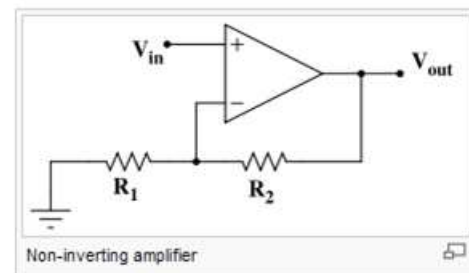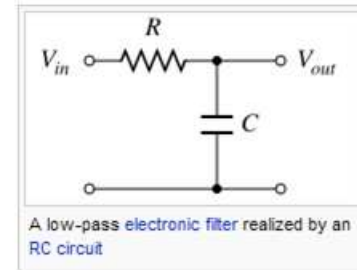
Chapter V: Detection Circuit

We needed to be able to tell when a cell was present in our system. For this we decided to design a detection circuit. This circuit would detect a cell by a modification in the light intensity. In order to design the detection circuit we started with a photodetector connected to a fiber optical cable by a ST connection
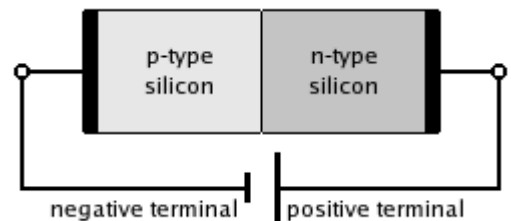
(OPF482). The light from an inferred LED goes into the microscope and then through the fiber optical cable into the photodetector. A photodetector is a photodiode which is a component with a p-n junction. When a photon, light, of sufficient energy strikes the diode, it excites an electron in the valence band thereby creating a mobile electron and a positively charged electron hole. If the absorption occurs in the junction's depletion region, or one diffusion length away from it, these carriers are swept from the junction by the built-in field of the depletion region, producing a photocurrent. Photodiodes can be used in either the zero bias mode, known as the photovoltaic mode, or in the reverse bias mode, known as the photoconductive mode, the mode we are interested in. In the zero bias mode, light striking the diode causes a current across the device which leads to a forward bias of the diode which in turn induces "dark current" in the opposite direction to the photocurrent. Dark current is the relatively small electric current that flows through a photodiode even when no photons are entering the device. This is called the photovoltaic effect and is the basis for how solar cells work, which are just a large number of big photodiodes. Onto reverse bias which only induces a little current (known as saturation or back

current) along its direction. But a more important effect of reverse bias is widening of the depletion layer (therefore expanding the reaction volume) and strengthening the photocurrent. Circuits based on this effect are more sensitive to light than ones based on the photovoltaic effect and also tend to have lower capacitance due to the greater separation of the charges, which improves the speed of their time response, because τ=RC so the smaller the capacitance the smaller the time constant. On the other hand, the photovoltaic mode tends to exhibit less

electronic noise. Another type of photodiodes is the avalanche photodiodes which have a similar structure, but are operated with a much higher reverse bias which allows each photo generated carrier to be multiplied by avalanche breakdown resulting in internal gain within the photodiode, which increases the effective responsively of the device. Our photodetector is used in reverse bias with a large resistor (1.8MΩ) to have the majority of the current flow into the circuit. The next step of the circuit is a low-pass filter with a cutoff frequency of 1,000 Hz to reduce the noise from the photodetector. The output from the filter goes into the operational amplifier or op-amp. The op-amp, a LF412CN, is setup in a non-inverting configuration with a gain (1 + R_2/R_1) of 2,500. After the op-amp stage, we have a voltage buffer or voltage follower, used as a buffer amplifier, which is used to eliminate loading effects or to interface impedances. $V_{out} = V_{in}$ with $Z_{in} = \infty$ in theory, but in reality it is the input impedance of the op-amp, which is usually 1MΩ to 1TΩ. Some of the difficulties we ran into were a noisy signal, which is why we added a low pass filter, having the op-amp osculate so we added some capacitors to eliminate this. We also had a week input signal which is why we increase the resistor to 1.8MΩ. Below is the final circuit.

A low-pass electronic filter realized by an RC circuit
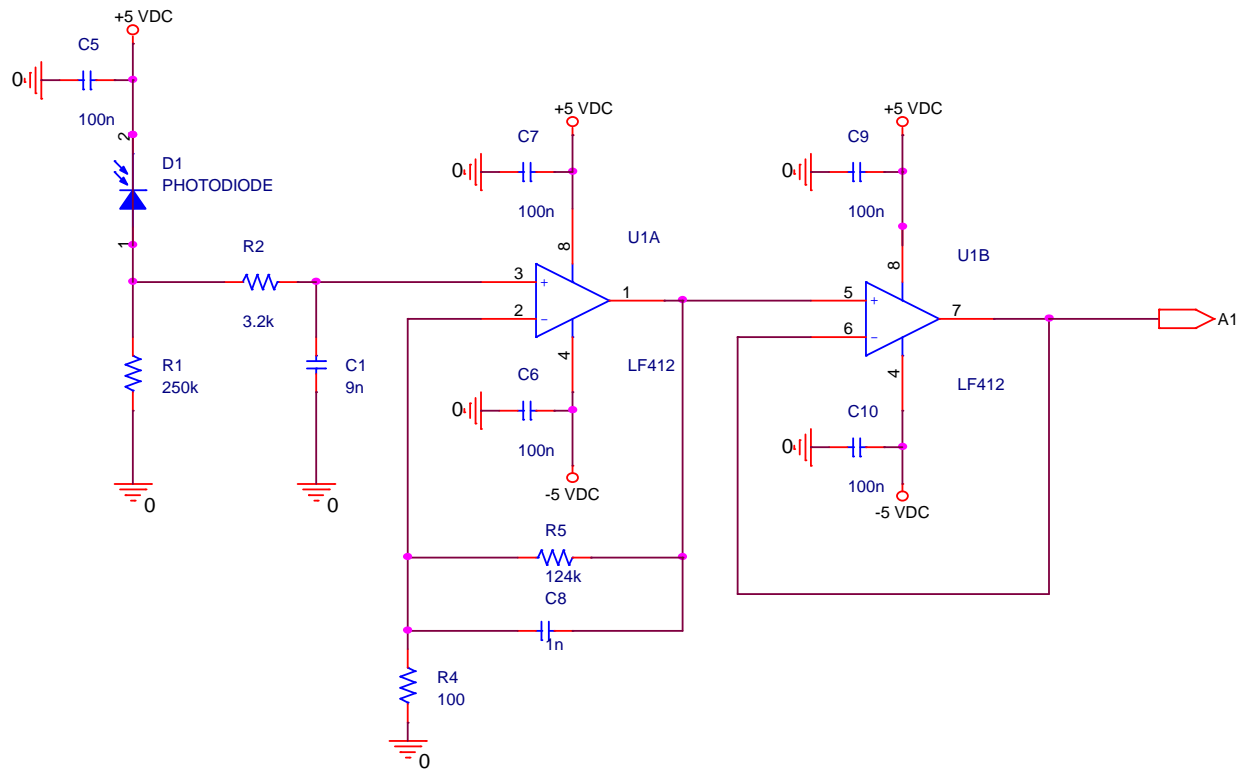

Non-inverting amplifier

Voltage follower

Figure 5.3

Chapter VI: Dielectrophoretic (DEP) Trapping

DEP trapping is necessary in this project for one main reason: If the sphere/cell/particle is not held in a particular position without moving, a spectral reading of light shined through that object will be extremely difficult to gather data with the equipment and limited budget that we have. DEP trapping is a method of using electromagnetic forces to hold an object in place. One might ask the question: how do you exert a force upon a neutral object using electromagnetics? The answer to this question is not trivial. DEP trapping occurs when a non-uniform electric field is passed through a neutral body. Internal to the neutral object, the molecules within the neutral object polarize, much like the depletion region that occurs when a voltage is put across a pn junction. The imbalance of localized charges results in a virtual electric dipole being formed within this neutral object. Therefore, the electric field will "apply" a force to this neutrally charged object. Since the objects we are concerned with are on the order of $10\,\mu m$ in diameter, it is easier to exert a significant enough force on these small particles to "push" them into a suitable area to take a spectral reading.
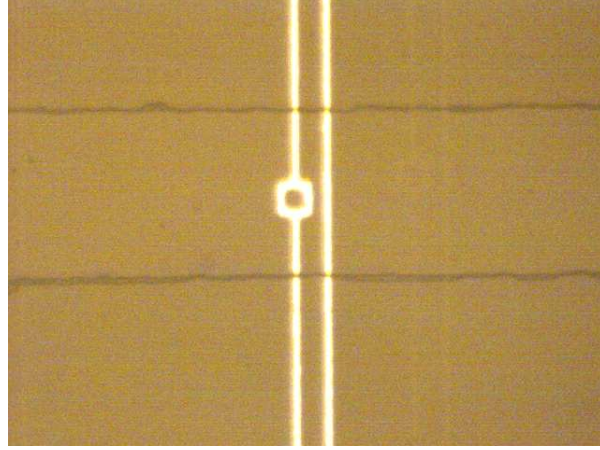
Figure 6.1 Picture of DEP trap electrodes

In order to achieve a non-uniform electric field, a time-varying voltage must be applied across the electrodes of the DEP trap. The approximate force applied to an object being trap can be defined by the formula:

$$\boldsymbol{F} = 2\pi\varepsilon_1 R^3 Re[\underline{CM}(\omega) \times \nabla\underline{\boldsymbol{E}}^2(\boldsymbol{r})] \qquad [1]$$

where F refers to the dipole approximation to the DEP force, ε_1 refers to the permittivity of the medium surrounding the object being trapped, R is the radius of the particle, r is the spatial coordinate, ω is the angular frequency of the applied voltage, E is the complex applied electric field, CM is the Claussius-Mossotti factor. The Clossius-Mossotti factor is a frequency dependent function of the permittivity of the medium outside the particle and the inside of the particle. In simpler terms, the force to push an object into a trap is proportional to the positional gradient of the electric field.

The implications of such a thing is that the particle will experience a force until it reaches an extrema in the intensity of the electric field (i.e. the positional derivative of the electric field is zero, and therefore the force will equal zero.) This translates into basically a restoring force that keeps the particle trapped at a certain point until the electric field is removed or until a much larger force physically removes the particle from the trapping area.

In the scope of this project, the non-uniform electric field comes from a 5 Vpp sinusoidal signal across the two electrodes of the traps.
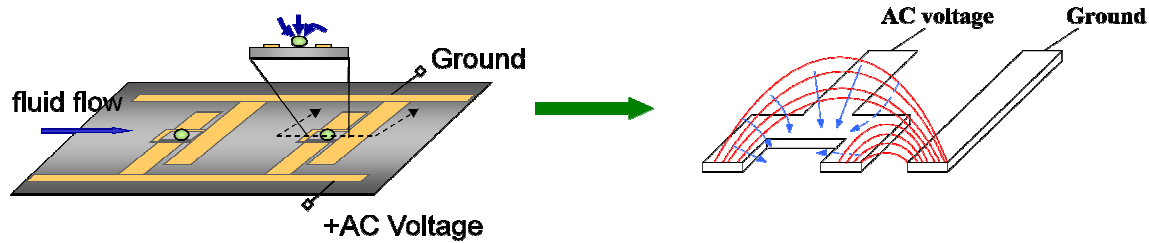
Figure 6.2 (a): Electromagnetic Modeling of DEP traps [2]

Based upon the field lines shown in figure 6 .2, the point of highest electric field intensity is approximately in the center of the trap. This provides an optimal trapping point for which the spectrometer can take a reading.

Chapters VII: Future Work

At the present time only PDMS channels are successful produced consistently for cell detection.   These channels can be implemented in trapping cells but makes cell differentiation due to frequency modulation impossible. A dielectric coated channel is required for differentiation. There are two solutions that must be established before a chip can both detect and differentiate cells. First, glass channels must be fabricated successfully on a consistent basis. New glass has been ordered to reduce the lattice impurities and hopefully will generate channels with uniform height. Second, an improved method for chip bonding must be discovered. Indium bonding has shown to be successful initially but at some costs. Depending on the thickness of the Indium layer, the channel can become leaky which could result in the loss of cells to outside the channel. Indium bonding also provides a weak bond. Under high pressure in the channel, the chip can break. Gold to gold bonding is the ideal method for bonding the two chips together and should be further researched.

The optical system needs to be fine tuned to allow the light modulation to focus on a smaller area. This will allow for more intensity modulation when a small object is in the focus area. If we are able to obtain any donations, a higher output infrared LED could improve the system. Also, if a high performance photo diode was obtained the optical detection circuit could be improved in the area of time response.

In the future of the project, the spectrometer will become a essential part of the cell analysis. Data acquisition will need to be automated using Labview software and resulting data of the cells will allow for cell differentiation. Because it is the shifting of the wavelength that differentiates cell types, the spectrometer is the heart of the system. Triggering DEP traps based

on light modulation (i.e. intensity) is very difficult and may not be feasible with current project limitations. An alternative to trapping based on light intensity would be to use the spectrometer and attempt to detect changes in wavelength and trigger the DEP traps accordingly. It may even be possible in the future to skip the trapping step entirely and simply take data of the cells' spectrums as they pass. Such alternatives will be investigated next semester along with other possibilities to improve the rate at which cells can be analyzed.

REFERENCES

http://www.optofluidics.caltech.edu/optofluidics/index.html
http://www.laserfocusworld.com/articles/article_display.html?id=259933
Wikipedia

[1] J. Voldman, R. Braff, M. Toner, M. Gray, and M. Schmidt, "Holding Forces of Single-Particle Dielectrophoretic Traps," *Biophysical Journal,* Vol. 80, pp 531-541, January 2001.

[2] W. Wang, H. Shao, K. Lear, *"Lab-on-a-Chip Single Particle Dielectrophoretic (DEP) Traps"* powerpoint presentation given *March 2006.*

[3] **Optofluidic Intracavity Spectroscopy of Canine Lymphoma and Lymphocytes**

Lear, Kevin L.; Shao, Hua; Wang, Weina; Lana, Susan E.;

LEOS Summer Topical Meetings, 2007 Digest of the IEEE, 23-25 July 2007 Page(s):121 – 122

APPENDIX OR APPENDICES

- **Appendix A: Abbreviations**

AC – Alternating Current

DAQ – Data Acquisition Unit

DC – Direct Current

DEP – Dielectrophoretic

LED – Light Emitting Diode

OFIS – Optofluidic Intracavity Spectroscopy

OpAmp – Operational Amplifier

PDMS – Polydimethylsiloxane

VI – Labview Virtual Instrument

Vpp – Volts Peak-to-Peak

- **Appendix B: Budget**

- ADG 452 Digital Switch -- $15
- Various circuit elements including Op-amps and digital chips -- $10
- Hytek iUSBDAQ U120816 -- $105
- TOTAL EXPENSES = $130

Starting Budget = $500 over 2 semesters

Money left = $500-$130=$370

With the remaining money, we will research things we can buy to optimize our system.

- **Appendix C: Peripherals**

The need for peripherals in this project is abundantly apparent. We used many different measurement and control systems to be able to achieve our goals. These peripherals were:

- Data Acquisition Unit (iUSBDAQ-U120816) from Hytek Automation

- Ocean Optics Spectrometer (HR2000)

- Oriel Instruments Encoder Mike Controller (18011)

- Microscope (heavily customized Olympus 230997)

- Logitech USB camera

- Beam splitter (Newport parts manufactured in-house)

C1: Data Acquisition Unit
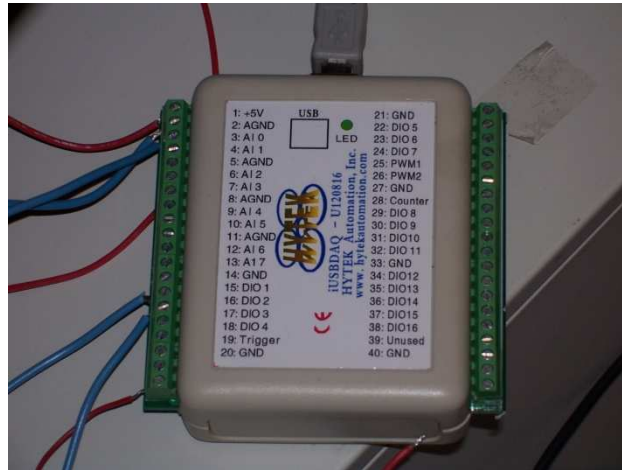
Figure C1.1 Hytek Data Acquisition Unit

The data acquisition unit was brought on board due to a need for triggering a circuit based on amount of light collected by the photodiode. This made it so that instead of creating a new logic circuit every time we changed the gain stage of the amplifier, the logic could be controlled with a Labview VI. This also took out the guess work for a logic chip. In the specification sheet for a 7400 series logic component, there was a large range of voltages that were specified to be undefined logic. The DAQ took a lot of the uncertainty out of the logic. The DAQ is accurate to within 3 mV DC on its 8 available channels of analog inputs. It also can output digital logic at 5 V DC on one of its 18 Digital I/O channels. This may seem like it's overkill to have so many, but the DAQ was 2/3 of the price of some of the other data acquisition units that are on the market. It has a sampling rate of 13,000 samples per second on a single channel. More expensive units were about the same or even worse. We designed a Labview VI that would take an analog input, compare it to some specified reference, and output a digital signal based upon whether or not it was higher or lower than the given reference.

Here is the front panel of the Labview VI:
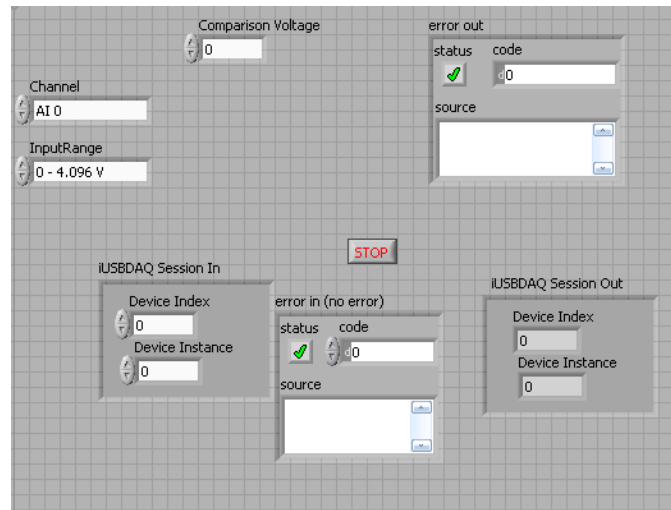
Figure C1.2 Front Panel of DAQ VI

The interface is quite simple. The triggering voltage is input in the field labeled "Comparison Voltage". The channel of the analog input is easily configured. Any errors are easily read on the error out field. Since we configured the DAQ to take inputs on analog channel 0 (the default value), getting a digital output based upon comparing to a preset voltage was as easy as inputting the comparison voltage, and hitting the run button in Labview.

The VI for controlling the DAQ was not difficult to program. Another reason we went with this DAQ was due to the fact that Labview VI's were available on the Hytek Automation website. This made it so that it was a "plug and chug" type of program. Here is the VI block diagram:
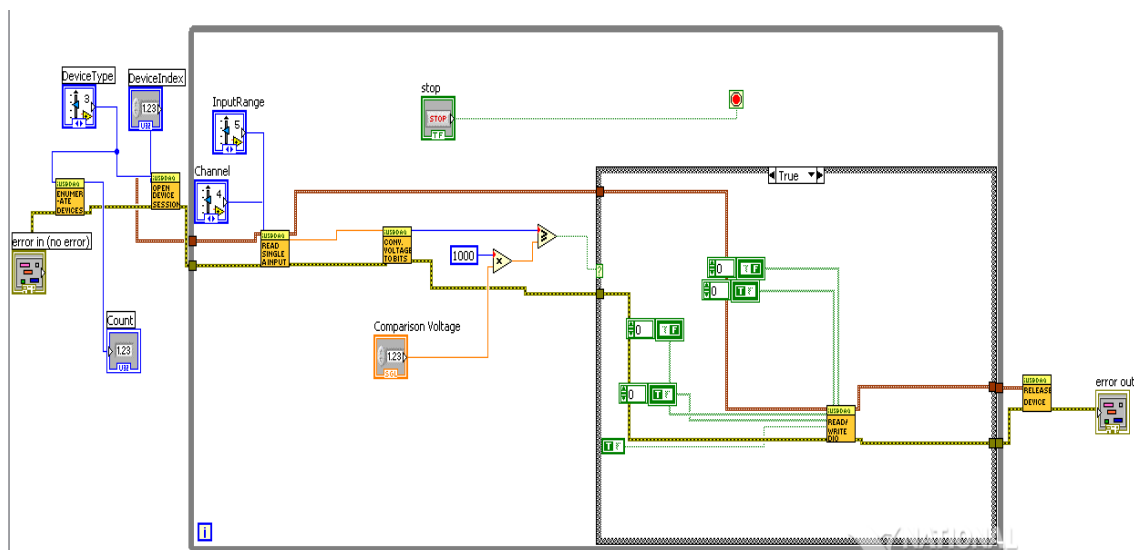
Figure C1.3 Block Diagram of DAQ VI

This block diagram shows all of the subVI's that were used to retrieve data from the DAQ, which were available on the Hytek website.

C2: Oriel Instruments Encoder Mike Controller 18011

<table>
<tr><td>(a)</td><td>(b)</td></tr>
</table>

Figure C.2.1(a) Control Panel of Oriel Controller (b) Microscope stage being controlled

The Oriel Instruments Encoder Mike Controller is normally used as a microscope stage controller to move a microscope stage very slowly. Our application of this piece of equipment was as a syringe pump. The main reason that this was used is because it was able to move a syringe plunger slow enough to get reasonably slow flow within the channel of the chip. The minimum rate at which the actuator can move is 0.5 µm/s. Remember that the chip only had a cross-sectional area of approximately 5000 μm^2. The syringe that we are using is approximately 0.5 cm in diameter. This makes it so that the stage must be moving extremely slow in order to get a flow rate within the channel to be as slow 40 µm per second, which is the flow rate by which it is suitable to trap cells. Again, we used Labview to control the actuator. This was much more difficult to control because there were no VIs available on the internet. This made for a much bigger challenge because we were unfamiliar with RS-232 communication that was required for control of the Oriel actuator. Using a wiring diagram that was in the User's manual of the Oriel actuator, we created our own RS-232 to DB9 cable to interface between the control panel and a computer.

Block Diagram

Labview program → DB9 → RS-232 → **Oriel Controller** → **Actuator** → **Syringe** → **Nanotube** → **Chip**

Set Parameters → **Pump?** → Yes → **On Cycle** → **Off Cycle** → **Stop?** → Yes → **Stop Pump**

Stop? → No
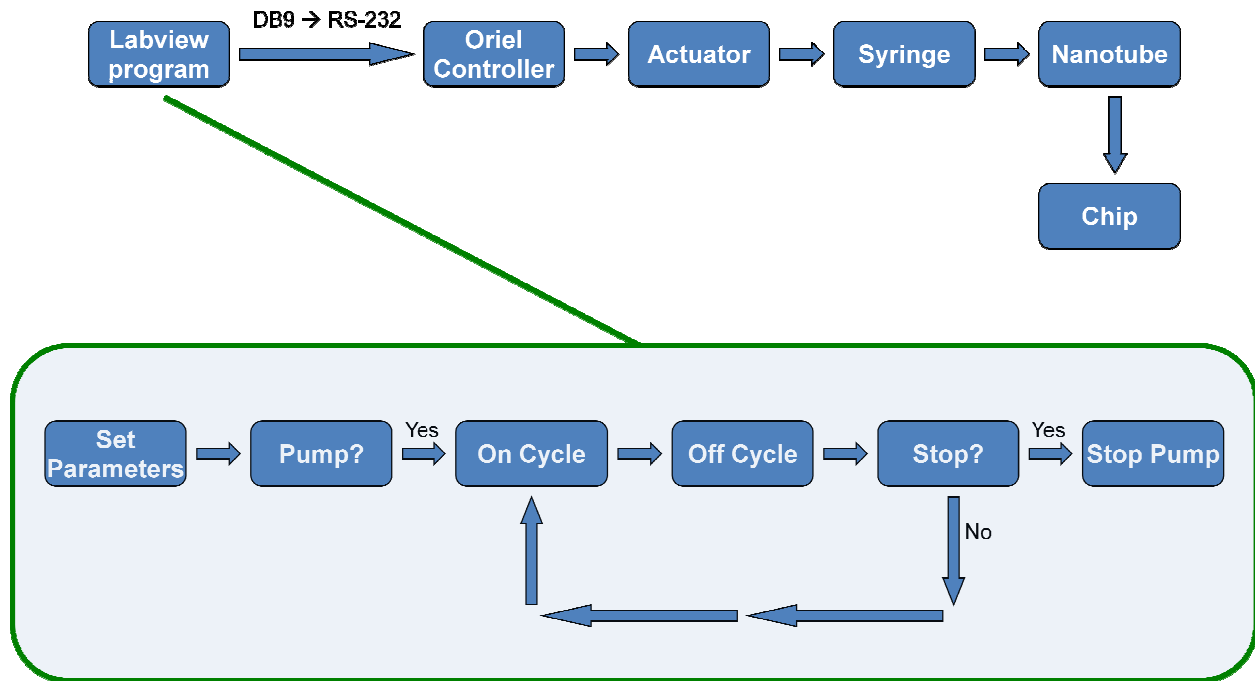
Figure C2.2

(a)   (b)

Figure C2.3(a)RS232 input to Oriel Controller

Figure C2.3(b) DB9 input to computer

A Labview VI controls the signals that are put on the different wires of the RS-232 Cable. The front panel for the Labview VI looks like this:
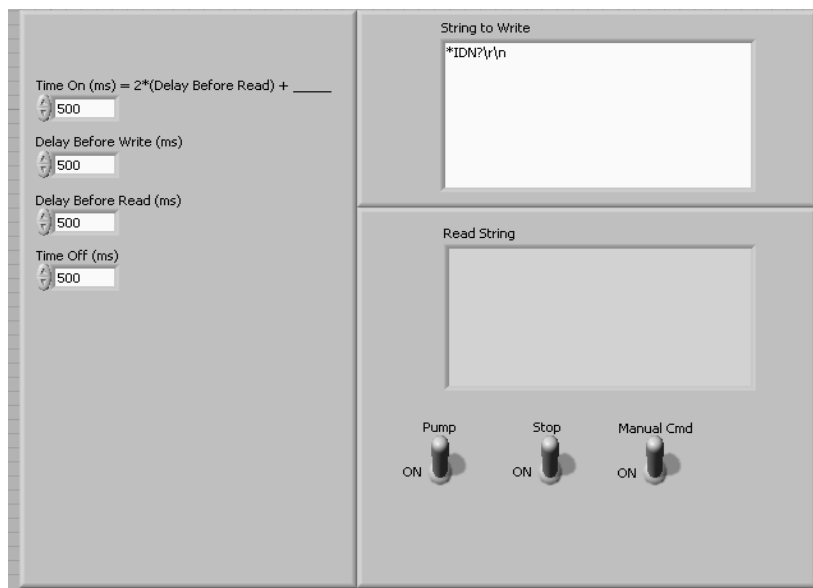
Figure C2.4 Front Panel of Oriel Controller VI

The switches in the lower right portion of the front panel control what the switch actually does. Only one switch can be on at one given time in order to function properly. When the VI is run with only the pump switch on, the pump will run for a total of 2*(Delay Before Read) + the time value(ms) specified in the top left input box. When the VI is run with the stop switch turned on, it will stop all pumping functions. With only the manual command switch turned on, a string will be sent to the Oriel controller. For example, the string "V200/n" will command the Oriel actuator to move at a velocity of 200 µm/second. There are many commands like this that the VI already uses to control the actuator within the VI itself, such as run and stop. The way that the pump command works is that it will send a run command. Then there will be a specified delay time, followed by the stop command being sent to the controller, then a second specified delay. The loop starts over starting with a run command. This allows the user to specify a duty cycle for the pump. The values that we used for this VI were: time on= 725 ms, delay before write = 50 ms, delay before read = 50 ms, and time off = 7000 ms. This roughly gave a flow rate of 40 µm per second. The VI block diagram shows all of the internal logic that occurs with the switches, and with the delays, as well as the Run and Stop commands sent to the Oriel actuator.

Figure C2.5

C3: Ocean Optics HR2000 High-Resolution Fiber Optic Spectrometer

The overall goal of the project is to differentiate cells as they pass through the channel. In order to do this, the method of intracavity spectroscopy will be used. In order to detect the changes in wavelength as a cell passes through, a spectrometer is used to analyze the diffraction of the LED light source. At this point in the project, the spectrometer has only been used to assist with the setup of the optical system. The spectrometer was used to maximize the light intensity from the LED light source as well as the focused LED light after it has passed through the lens. The resulting spectrum also provided verification that the microscope optics were properly aligned. Narrow peaks in the spectrum indicated proper alignment from the LED light source to the microscope.

C4: Optical Calibration

At the heart of the OFIS process is the microscope. This is the instrument that we use to gather light to use for spectroscopy, cell detection, and for the camera. No other instrument needs to be calibrated as frequently as the microscope, and no other instrument in the process can dramatically change the resulting data by a slight adjustment. Therefore the correct calibration of both the microscope and the light source is vital for any reasonable data collection from a micro-fluidic sample. In this section, the calibration process of the microscope will be covered. The difficulties in learning how to calibrate the microscope will also be explored.

To begin, the basic knowledge of how our system works is essential. Below, is a figure on the general set up of the entire system. The size of the optic fiber coupled into the beam splitter should be around 50/125 to 62.5/125, and needs to be a multimode fiber. The percentage of light sent through the optic fiber is 90%, while the remaining 10% of light goes to a camera. To calibrate the microscope, the use of a LED that emits light in the visible spectrum is crucial, as well as a focusing lens above the LED and below the microscope's focus plane. By placing a white piece of paper on the focusing plane, the microscope is focused while the focusing lens for the LED is also focused on the same plane. The goal of the lens above the LED is to make the light emitted from the LED confined to a very small area in a circular shape.

Figure C4.1: Diagram of microscope being coupled with light source

The piece of paper is then removed, and the microscope stage is then positioned over the emitted LED light until the LED light is centered in the middle of the viewing plane. The microscope light is then turned off, and an alignment laser in the infrared region is transmitted into the viewing plane through an optic fiber. Light from the laser is seen in the viewing plane, and the output from the beam splitter is adjusted until the laser light is confined to a small area as well as centered over the emitted LED light. This ensures that the output from the beam splitter is collecting light from where the LED light is focused on.

Figure C4.2: Example of alignment using a

The difficulties encountered in the calibration of the microscope were numerous, and were mainly due to the poor maintenance of the entire instrument. The second difficulty is the basic concept of the optics.

The microscope used for our experiments has been poorly maintained. Dirt and scratches on the lens are present, which may alter the light collection, but to a lesser degree. The beam splitter stage was unstable and poorly fitted onto the microscope, and due to budget constraints has to be fastened to the microscope with zip ties. If our budget constraints allow, we can machine better housing for the beam splitter. The focusing plane where the micro-fluidic channels sit is also difficult to use with the channels. Scotch tape is required to steady the chip in place and leveled with the focusing plane. The use of tape leads to oils from the fingers being deposited onto the chip, which alters the light characteristics of the chip. Again, if our budget would allow, we could machine a better focusing plane that would allow us to secure the chip into place and avoid taping it. The fiber optic output from the beam splitter is also difficult to use at time, as there is no relief at the ST junction for the fiber optic cable. A relief at the ST junction would allow for the focal length from the optic fiber to the beam splitter to be changed without causing stress to the fiber optic cable or having to dissemble the output of the beam splitter.

The knowledge of optics was one of the easier difficulties to overcome with the help of Dr. Lear. Understanding why we needed a 62.5/125 optic fiber as opposed to a much larger optic fiber is an example of the problems he helped us overcome. The reason why a 62.5/125 cable is used to minimize the area in which the light from the beams splitter is collected.

- Appendix D: Data Sheets and User Manuals

D1: OPF 482 Optic Fiber Photodiode

⊗ OPTEK

Fiber Optic High Speed PIN Photodiode in ST* Receptacle
Type OPF482

DIMENSIONS ARE IN INCHES (MILLIMETERS)
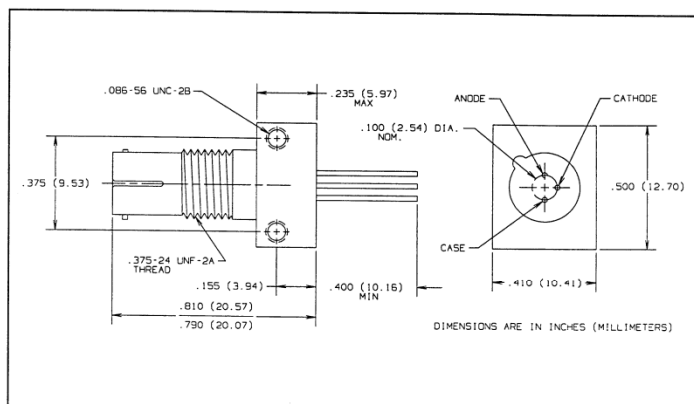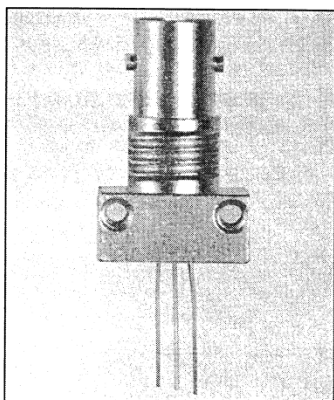
Features

- Component pre-mounted and ready to use
- High speed, low capacitance
- Pre-tested with fiber to assure performance
- Popular ST style receptacle
- Electronically isolated from case

Description

The OPF482 consists of a low cost plastic cap PIN photodiode pre-mounted and aligned in an ST receptacle. This configuration is designed for PC board or panel mounting. Includes lock washer and jam nut, two 2-56 screws, and dust cap.

The PIN Photodiodes are designed to interface with multimode optical fibers from 50/125 to 100/140 microns.

*ST is a registered trademark of AT&T.

Absolute Maximum Ratings ($T_A = 25^\circ$ C unless otherwise noted)

Reverse Voltage . . . . 100 VDC
Continuous Power Dissipation . . . . 200 mW[1]
Storage Temperature Range . . . . -55° C to $+100^\circ$ C
Operating Temperature Range . . . . -40° C to $+85^\circ$ C
Lead Soldering Temperature [1/16 inch (1.6 mm) from case for 5 sec. with soldering iron] . . . . 240° C[2]

Notes:
(1) Derate linearly @ 2.0 mW/$^\circ$ C above 25° C.
(2) RMA flux is recommended. Duration can be extended to 10 sec. max when flow soldering.
(3) Test @ V_R = 5 V with 50/125 micron, 0.20 N.A. fiber, @ 10 μW optical power @ 850 nm. Responsivity levels apply to 50 μm, 62.5 μm and 100 μm core optical fibers.

Type OPF482

Electrical Characteristics ($T_A = 25^\circ$ C unless otherwise noted)

SYMBOL	PARAMETER	MIN	TYP	MAX	UNITS	TEST CONDITIONS
R	Flux Responsivity	0.45	0.55		A/W	$V_R = 5.0$ V[3]
I_D	Dark Current		0.1	5.0	nA	$V_R = 5.0$ V
λp	Peak Response Wavelength		860		nm	
t_r	Output Rise Time		0.6		ns	$V_R = 50$ V, $R_L = 50\ \Omega$, 10%-90%
t_r	Output Rise Time		1.0		ns	$V_R = 15$ V, $R_L = 50\ \Omega$, 10%-90%
t_r	Output Rise Time		2.0		ns	$V_R = 5.0$ V, $R_L = 50\ \Omega$, 10%-90%
C_T	Total Capacitance		1.5	2.0	pF	$V_R = 5.0$ V

Typical Performance Curves
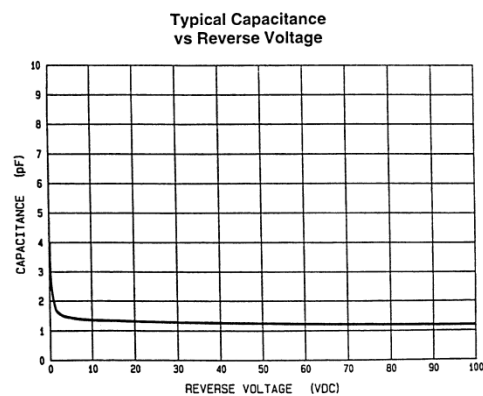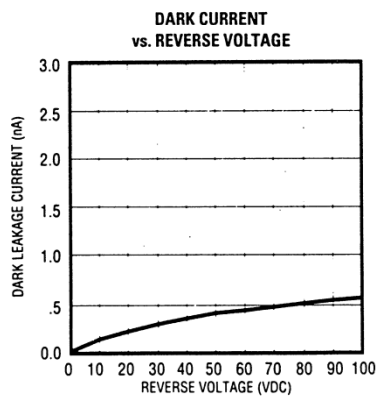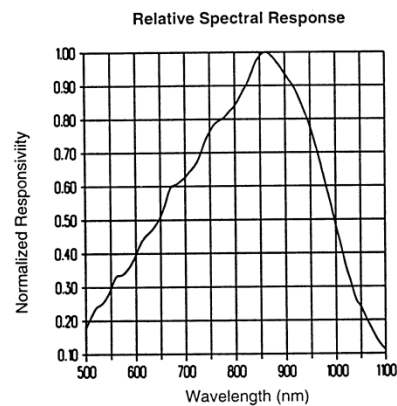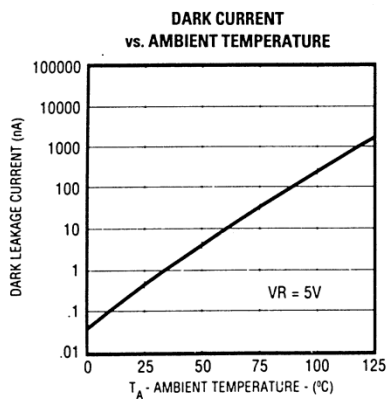
DARK CURRENT vs. AMBIENT TEMPERATURE

Relative Spectral Response

DARK CURRENT vs. REVERSE VOLTAGE

Typical Capacitance vs Reverse Voltage

8-91

FIBER OPTIC COMPONENTS

28

D2: DAQ Comparison

	Number of Channels:	Measurement range:
DI-148U	8	±10V
DI-158	4	Variable - Depends on internal gain setting
NI USB-6008	8	±20V
LabJack U3	16	±2.4(?)
iUSBDAQ – U120816	8	0-4.096V
For minimum required digital I/O I required a minimum logic high voltage of 2V		
and a max logic low voltage of 0.8V		
To even consider a device, I first looked to see if it had LabView drivers. I then had		
a price cutoff of $150-160.		
A/D Characteristics		
Resolution:	Conversion Time:	Max. throughput sample rate
10-bit	70µs	14400 [Hz]
12-bit		14400 [Hz]
12-bit		10 [kS/s]
12-bit		2.5-50 [kS/s]
12-bit		32 [kS/s]
	Digital I/O	
Channels	Mininum Required Digital I/O?	Labview
6 bi-directional ports	Yes	Labview 5
4 bi-directional ports	Yes	Labview 5
12	Yes	Yes
20 (Programmable Ports)	Yes	Yes
16 bi-directional ports	Yes	Yes
Cost		
$50		
$99		
$159		
$99		
$86		

D3:LF412 Operational Amplifier

National Semiconductor

August 2000

LF412
Low Offset, Low Drift Dual JFET Input Operational Amplifier

General Description

These devices are low cost, high speed, JFET input operational amplifiers with very low input offset voltage and guaranteed input offset voltage drift. They require low supply current yet maintain a large gain bandwidth product and fast slew rate. In addition, well matched high voltage JFET input devices provide very low input bias and offset currents. The LF412 dual is pin compatible with the LM1558, allowing designers to immediately upgrade the overall performance of existing designs.

These amplifiers may be used in applications such as high speed integrators, fast D/A converters, sample and hold circuits and many other circuits requiring low input offset voltage and drift, low input bias current, high input impedance, high slew rate and wide bandwidth.

Features

- Internally trimmed offset voltage: 1 mV (max)
- Input offset voltage drift: 10 μV/°C (max)
- Low input bias current: 50 pA
- Low input noise current: 0.01 pA/$\sqrt{Hz}$
- Wide gain bandwidth: 3 MHz (min)
- High slew rate: 10V/μs (min)
- Low supply current: 1.8 mA/Amplifier
- High input impedance: $10^{12}\Omega$
- Low total harmonic distortion: ≤0.02%
- Low 1/f noise corner: 50 Hz
- Fast settling time to 0.01%: 2 μs

Typical Connection
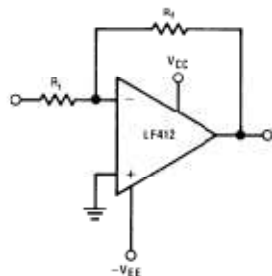
00565641

Ordering Information

LF412XYZ

X indicates electrical grade

Y indicates temperature range
  "M" for military
  "C" for commercial

Z indicates package type
  "H" or "N"

Connection Diagrams

Metal Can Package

Note: Pin 4 connected to case.
TOP VIEW
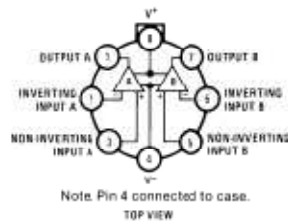
00565642

**Order Number LF412MH, LF412CH
or LF412MH/883 (Note 1)
See NS Package Number H08A**

Dual-In-Line Package
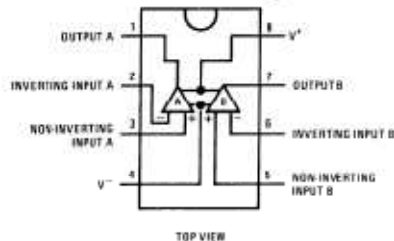
TOP VIEW

00565644

**Order Number LF412ACN, LF412CN
or LF412MJ/883 (Note 1)
See NS Package Number J08A or N08E**

D-FET II™ is a trademark of National Semiconductor Corporation.

© 2004 National Semiconductor Corporation   DS005656

www.national.com

Simplified Schematic

1/2 Dual

00565042
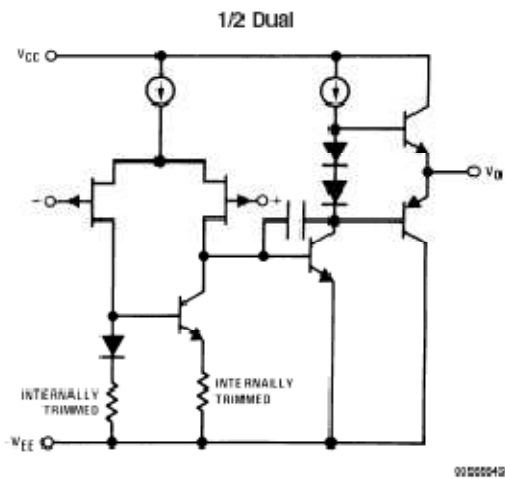
Note 1: Available per JM38510/11905

Detailed Schematic

00565032

2

31
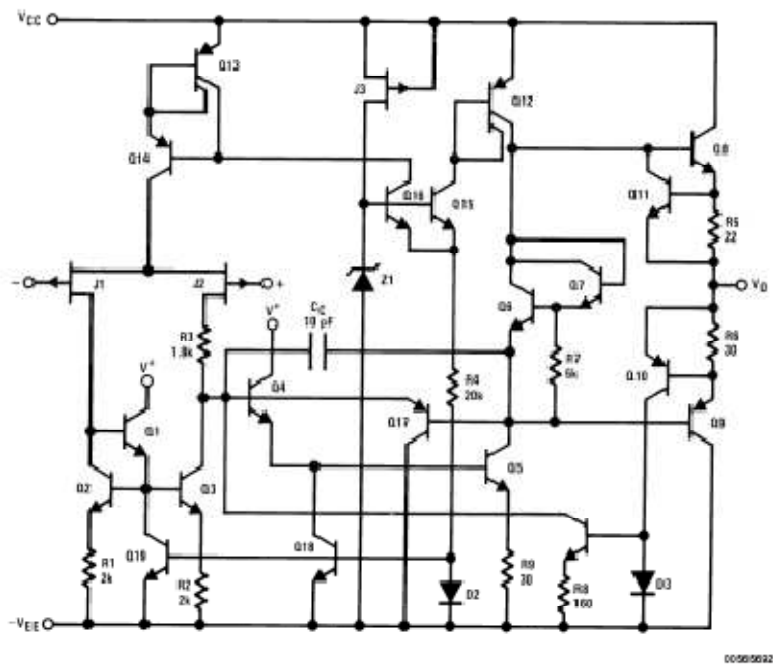
Absolute Maximum Ratings (Note 2)

If Military/Aerospace specified devices are required, please contact the National Semiconductor Sales Office/Distributors for availability and specifications.

(Note 11)

	LF412A	LF412
Supply Voltage	±22V	±18V
Differential Input Voltage	±38V	±30V
Input voltage Range		
(Note 3)	±19V	±15V
Output Short Circuit		
Duration (Note 4)	Continuous	Continuous
	H Package	N Package

Power Dissipation

		H Package	N Package
(Note 12)		(Note 5)	670 mW
T_J max		150°C	115°C
θ_{JA} (Typical)		152°C/W	115°C/W
Operating Temp. Range		(Note 6)	(Note 6)
Storage Temp.		−65°C≤T_A≤150°C	−65°C≤T_A≤150°C
Range			
Lead Temp.			
(Soldering, 10 sec.)		260°C	260°C
ESD Tolerance			
(Note 13)		1700V	1700V

DC Electrical Characteristics

(Note 7)

Symbol	Parameter	Conditions		LF412A			LF412			Units
				Min	Typ	Max	Min	Typ	Max	
V_{OS}	Input Offset Voltage	R_S=10 kΩ, T_A=25°C			0.5	1.0		1.0	3.0	mV
$\Delta V_{OS}/\Delta T$	Average TC of Input Offset Voltage	R_S=10 kΩ (Note 8)			7	10		7	20	µV/°C
I_{OS}	Input Offset Current	V_S=±15V	T_J=25°C		25	100		25	100	pA
		(Notes 7, 9)	T_J=70°C			2			2	nA
			T_J=125°C			25			25	nA
I_B	Input Bias Current	V_S=±15V	T_J=25°C		50	200		50	200	pA
		(Notes 7, 9)	T_J=70°C			4			4	nA
			T_J=125°C			50			50	nA
R_{IN}	Input Resistance	T_J=25°C			10^{12}			10^{12}		Ω
A_{VOL}	Large Signal Voltage Gain	V_S=±15V, V_O=±10V, R_L=2k, T_A=25°C		50	200		25	200		V/mV
		Over Temperature		25	200		15	200		V/mV
V_O	Output Voltage Swing	V_S=±15V, R_L=10k		±12	±13.5		±12	±13.5		V
V_{CM}	Input Common-Mode Voltage Range			±16	+19.5		±11	+14.5		V
					−16.5			−11.5		V
CMRR	Common-Mode Rejection Ratio	R_S≤10k		80	100		70	100		dB
PSRR	Supply Voltage Rejection Ratio	(Note 10)		80	100		70	100		dB
I_S	Supply Current	V_O = 0V, R_L = ∞			3.6	5.6		3.6	6.5	mA

Note 2: "Absolute Maximum Ratings" indicate limits beyond which damage to the device may occur. Operating Ratings indicate conditions for which the device is functional, but do not guarantee specific performance limits.

AC Electrical Characteristics

(Note 7)

Symbol	Parameter	Conditions		LF412A			LF412			Units
				Min	Typ	Max	Min	Typ	Max	
	Amplifier to Amplifier Coupling	T_A=25°C, f=1 Hz-20 kHz (Input Referred)			−120			−120		dB
SR	Slew Rate	V_S=±15V, T_A=25°C		10	15		8	15		V/µs
GBW	Gain-Bandwidth Product	V_S=±15V, T_A=25°C		3	4		2.7	4		MHz

AC Electrical Characteristics (Continued)

(Note 7)

Symbol	Parameter	Conditions	LF412A			LF412			Units
			Min	Typ	Max	Min	Typ	Max	
THD	Total Harmonic Dist	A_V=+10, R_L=10k, V_O=20 Vp-p, BW=20 Hz-20 kHz		≤0.02			≤0.02		%
e_n	Equivalent Input Noise Voltage	T_A=25°C, R_S=100Ω, f=1 kHz		25			25		nV/$\sqrt{Hz}$
i_n	Equivalent Input Noise Current	T_A=25°C, f=1 kHz		0.01			0.01		pA/$\sqrt{Hz}$

Note 3: Unless otherwise specified the absolute maximum negative input voltage is equal to the negative power supply voltage.

Note 4: Any of the amplifier outputs can be shorted to ground indefinitely, however, more than one should not be simultaneously shorted as the maximum junction temperature will be exceeded.

Note 5: For operating at elevated temperature, these devices must be derated based on a thermal resistance of $θ_{JA}$.

Note 6: These devices are available in both the commercial temperature range 0°C≤T_A≤70°C and the military temperature range −55°C≤T_A≤125°C. The temperature range is designated by the position just before the package type in the device number. A "C" indicates the commercial temperature range and an "M" indicates the military temperature range. The military temperature range is available in "H" package only. In all cases the maximum operating temperature is limited by internal junction temperature T_J max.

Note 7: Unless otherwise specified, the specifications apply over the full temperature range and for V_S=±20V for the LF412A and for V_S=±15V for the LF412. V_{OS}, I_B, and I_{OS} are measured at V_{CM}=0.

Note 8: The LF412A is 100% tested to this specification. The LF412 is sample tested on a per amplifier basis to insure at least 85% of the amplifiers meet this specification.

Note 9: The input bias currents are junction leakage currents which approximately double for every 10°C increase in the junction temperature, T_J. Due to limited production test time, the input bias currents measured are correlated to junction temperature. In normal operation the junction temperature rises above the ambient temperature as a result of internal power dissipation, P_D. T_J=T_A+$θ_{JA}$ P_D where $θ_{JA}$ is the thermal resistance from junction to ambient. Use of a heat sink is recommended if input bias current is to be kept to a minimum.

Note 10: Supply voltage rejection ratio is measured for both supply magnitudes increasing or decreasing simultaneously in accordance with common practice. V_S = ±6V to ±15V.
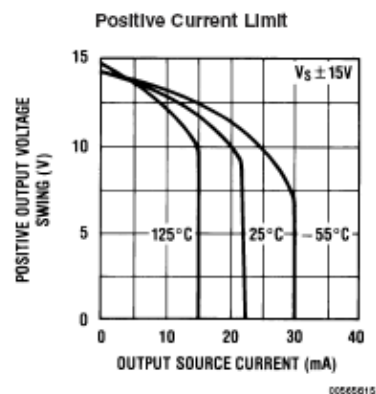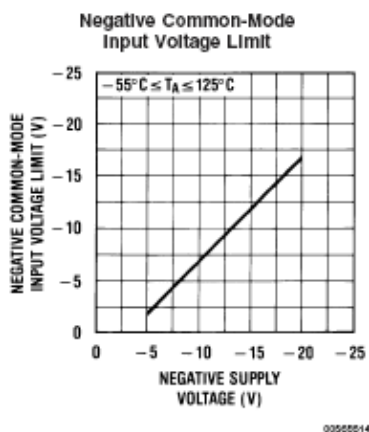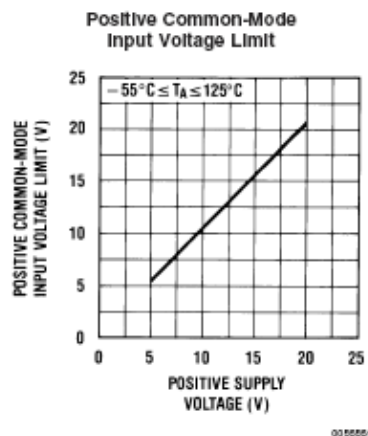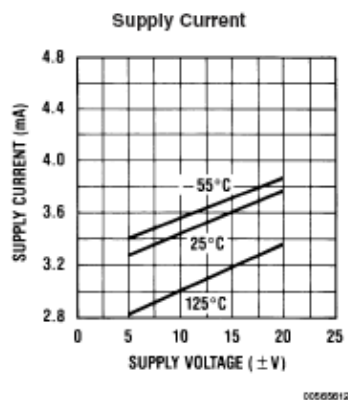
Note 11: Refer to RETS412X for LF412MH and LF412MJ military specifications.

Note 12: Max. Power Dissipation is defined by the package characteristics. Operating the part near the Max. Power Dissipation may cause the part to operate outside guaranteed limits.
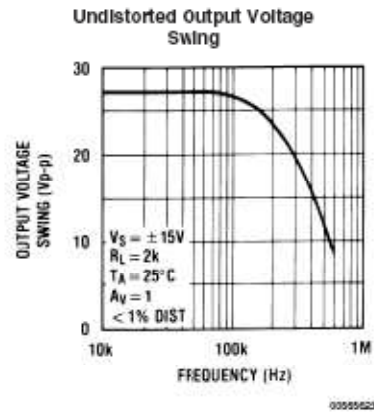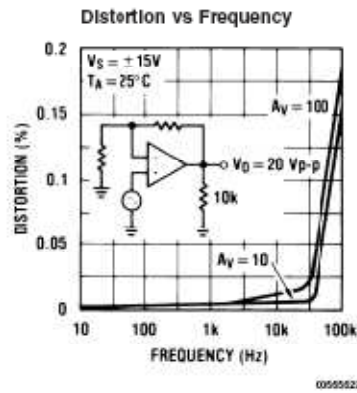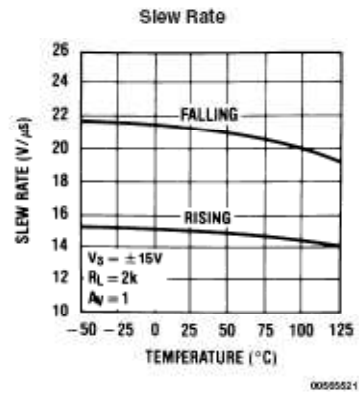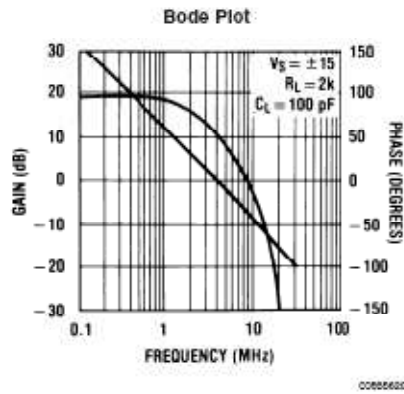
Note 13: Human body model, 1.5 kΩ in series with 100 pF.

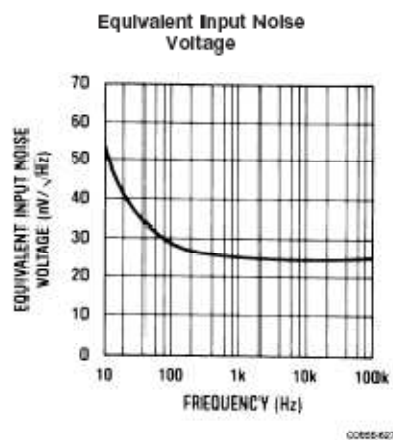## Typical Performance Characteristics
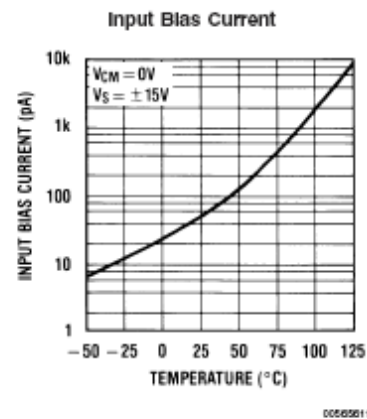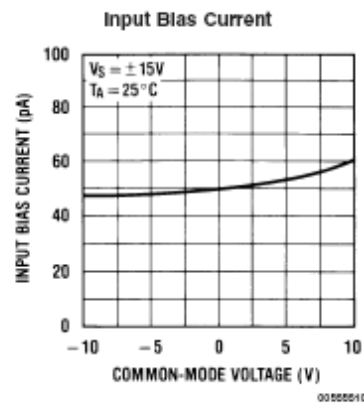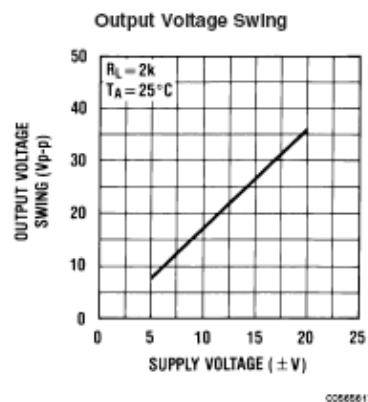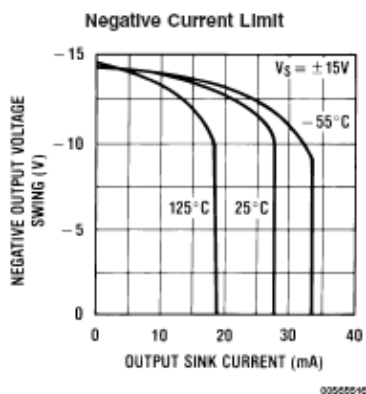
Input Bias Current

Input Bias Current

Typical Performance Characteristics (Continued)

Supply Current

Positive Common-Mode Input Voltage Limit

Negative Common-Mode Input Voltage Limit

Positive Current Limit

Negative Current Limit

Output Voltage Swing

5

34

Typical Performance Characteristics (Continued)

Output Voltage Swing

Gain Bandwidth

Bode Plot

Slew Rate

Distortion vs Frequency

Undistorted Output Voltage Swing

35

Typical Performance Characteristics (Continued)

Open Loop Frequency Response

00565624

Common-Mode Rejection Ratio

00565625

Power Supply Rejection Ratio

00565626

Equivalent Input Noise Voltage

00565627

Open Loop Voltage Gain

00565628

Output Impedance

00565629

7

36

Typical Performance Characteristics (Continued)

Inverter Settling Time

Pulse Response $R_L=2$ kΩ, $C_L=10$ pF

Small Signal Inverting

Small Signal Non-Inverting

Large Signal Inverting

Large Signal Non-Inverting

37

Pulse Response R_L=2 kΩ, C_L=10 pF (Continued)

Current Limit (R_L=100Ω)

TIME (5 µs/DIV)
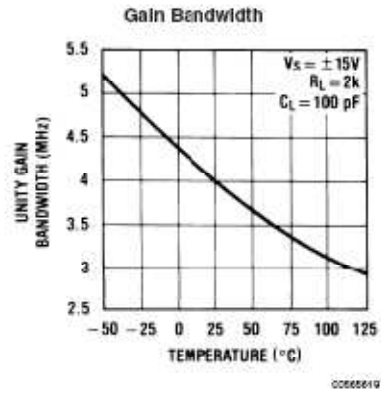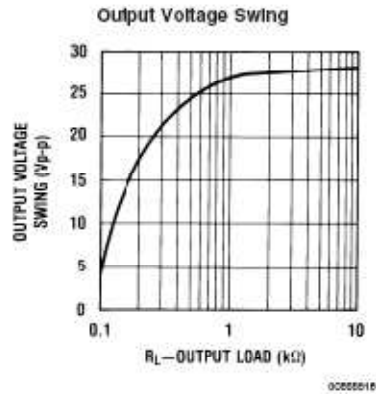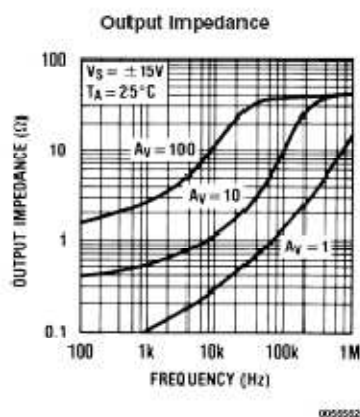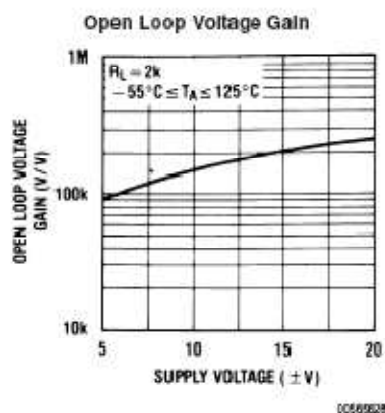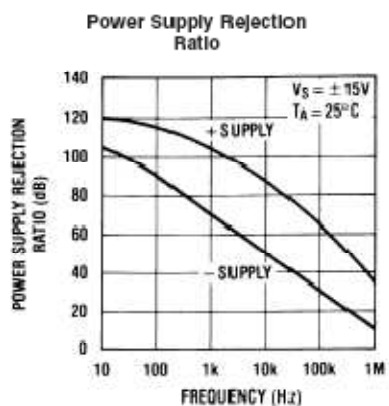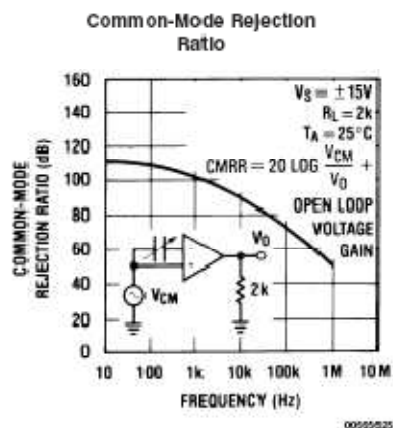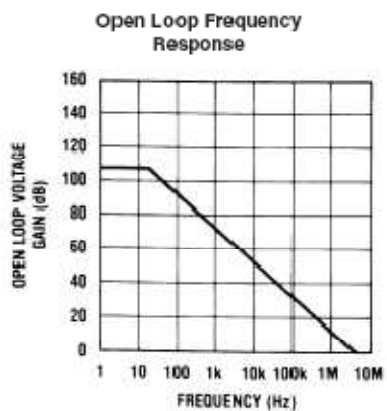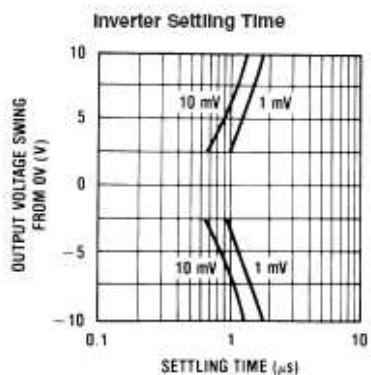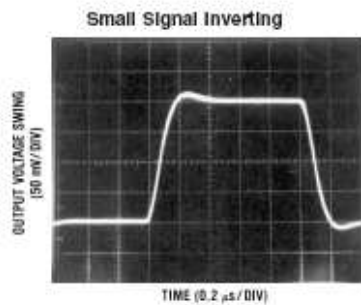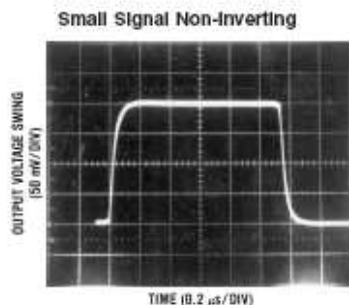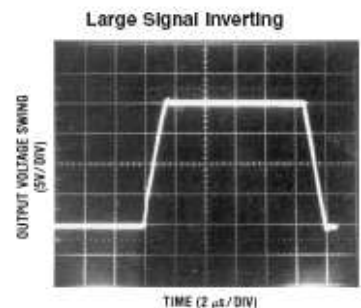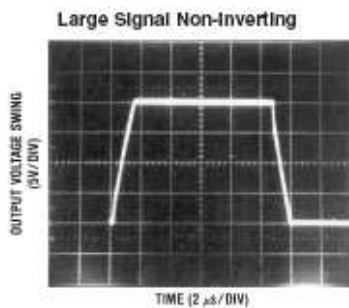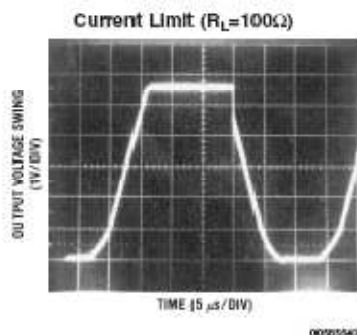
Application Hints

The LF412 series of JFET input dual op amps are internally trimmed (BI-FET II™) providing very low input offset voltages and guaranteed input offset voltage drift. These JFETs have large reverse breakdown voltages from gate to source and drain eliminating the need for clamps across the inputs. Therefore, large differential input voltages can easily be accommodated without a large increase in input current. The maximum differential input voltage is independent of the supply voltages. However, neither of the input voltages should be allowed to exceed the negative supply as this will cause large currents to flow which can result in a destroyed unit.

Exceeding the negative common-mode limit on either input will cause a reversal of the phase to the output and force the amplifier output to the corresponding high or low state.

Exceeding the negative common-mode limit on both inputs will force the amplifier output to a high state. In neither case does a latch occur since raising the input back within the common-mode range again puts the input stage and thus the amplifier in a normal operating mode.

Exceeding the positive common-mode limit on a single input will not change the phase of the output, however, if both inputs exceed the limit, the output of the amplifier may be forced to a high state.

The amplifiers will operate with a common-mode input voltage equal to the positive supply; however, the gain bandwidth and slew rate may be decreased in this condition. When the negative common-mode voltage swings to within 3V of the negative supply, an increase in input offset voltage may occur.

Each amplifier is individually biased by a zener reference which allows normal circuit operation on ±6.0V power supplies. Supply voltages less than these may result in lower gain bandwidth and slew rate.

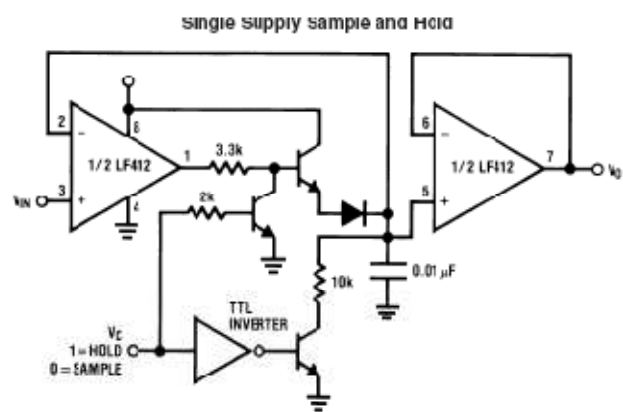The amplifiers will drive a 2 kΩ load resistance to ±10V over the full temperature range. If the amplifier is forced to drive heavier load currents, however, an increase in input offset voltage may occur on the negative voltage swing and finally reach an active current limit on both positive and negative swings.
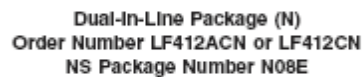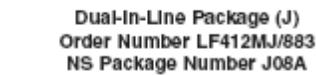
Precautions should be taken to ensure that the power supply for the integrated circuit never becomes reversed in polarity or that the unit is not inadvertently installed backwards in a socket as an unlimited current surge through the resulting forward diode within the IC could cause fusing of the internal conductors and result in a destroyed unit.

As with most amplifiers, care should be taken with lead dress, component placement and supply decoupling in order to ensure stability. For example, resistors from the output to an input should be placed with the body close to the input to minimize "pick-up" and maximize the frequency of the feedback pole by minimizing the capacitance from the input to ground.

A feedback pole is created when the feedback around any amplifier is resistive. The parallel resistance and capacitance from the input of the device (usually the inverting input) to AC ground set the frequency of the pole. In many instances the frequency of this pole is much greater than the expected 3 dB frequency of the closed loop gain and consequently there is negligible effect on stability margin. However, if the feedback pole is less than approximately 6 times the expected 3 dB frequency a lead capacitor should be placed from the output to the input of the op amp. The value of the added capacitor should be such that the RC time constant of this capacitor and the resistance it parallels is greater than or equal to the original feedback pole time constant.

Typical Application

Single Supply Sample and Hold

39

Physical Dimensions inches (millimeters) unless otherwise noted (Continued)

R0.010 TYP
R0.025 TYP

0.400 MAX

0.220
0.291

0.310 MAX
GLASS

0.045
0.065 TYP

0.005 MIN

GLASS SEALANT

0.020
0.060

0.200 MAX

0.125
0.200

0.150 MIN

0.290
0.320

0.180 MAX

95° ± 5° TYP

0.310
0.410

0.008
0.012 TYP

0.055 MAX
BOTH ENDS

90° ± 4° TYP

0.018 ± 0.003 TYP

0.100 ± 0.010 TYP

J08A (REV K)

Dual-In-Line Package (J)
Order Number LF412MJ/883
NS Package Number J08A

0.373 – 0.400
(9.474 – 10.16)

0.090
(2.286)

0.092
(2.337) DIA

PIN NO. 1 IDENT

OPTION 1

0.250 ± 0.005
(6.35 ± 0.127)

0.032 ± 0.005
(0.813 ± 0.127) RAD

PIN NO. 1 IDENT

OPTION 2

0.280
(7.112) MIN

0.300 – 0.320
(7.62 – 8.128)

0.030
(0.762) MAX

0.040
(1.016) TYP

0.039
(0.991)

20° ± 1°

0.145 – 0.200
(3.683 – 5.080)

0.130 ± 0.005
(3.302 ± 0.127)

95° ± 5°

0.009 – 0.015
(0.229 – 0.381)

0.125
(3.175) DIA NOM

0.325 +0.040 −0.015
(8.255 +1.016 −0.381)

0.065
(1.651)

90° ± 4° TYP

0.125 – 0.140
(3.175 – 3.556)

0.020
(0.508) MIN

0.018 ± 0.003
(0.457 ± 0.076)

0.100 ± 0.010
(2.540 ± 0.254)

0.045 ± 0.015
(1.143 ± 0.381)

0.050
(1.270)

0.060
(1.524)

N08E (REV F)

Dual-In-Line Package (N)
Order Number LF412ACN or LF412CN
NS Package Number N08E

40

D4: Relevant Syringe Pump User Manual Page

12.7 Syringe Diameters and Rate Limits

Manufacturer	Syringe (cc)	Inside Diameter (mm)	Maximum Rate (mL/hr)	Minimum Rate (µl/hr)
B-D	1	4.699	53.07	0.73
	3	8.585	177.1	2.434
	5	11.99	345.5	4.748
	10	14.43	500.4	6.876
	20	19.05	872.2	11.99
	30	21.59	1120	15.4
	60	26.59	1699	23.35
HSW	1	4.69	52.86	0.727
Norm-Ject	3	9.65	223.8	3.076
	5	12.45	372.5	5.119
	10	15.9	607.6	8.349
	20	20.05	956.2	13.28
	30	22.9	1260	17.32
	50	29.2	2049	28.16
Monoject	1	5.74	79.18	1.088
	3	8.941	192.1	2.64
	6	12.7	387.6	5.326
	12	15.72	593.9	8.161
	20	20.12	972.9	13.37
	35	23.52	1329	18.27
	60	26.64	1705	23.44
Terumo	1	4.7	53.09	0.73
	3	8.95	192.5	2.646
	5	13	406.1	5.581
	10	15.8	600	8.244
	20	20.15	975.8	13.41
	30	23.1	1282	17.63
	60	29.7	2120	29.13
Air-Tite	10	15.9	607.6	8.349
	20	20.25	935.5	13.55
	30	22.5	1216	16.72
	50	29	2021	27.78

	Syringe (uL)	Inside Diameter (mm)	Maximum Rate (ul/hr)	Minimum Rate (µl/hr)
Hamilton Microliter	0.5	0.103	25.49	0.001
	1	0.146	51.23	0.001
	2	0.206	101.9	0.002
	5	0.326	255.4	0.004
SGE	0.5	0.1	24.03	0.001
	1	0.15	54.07	0.001

D5: Infrared LED

LED

Infrared LED
L2791 series

Small emission spot LED using current confined chip

L2791 is infrared LED with a microball lens cemented to the current confined chip surface. This combination ensures high directivity and improved emission uniformity. In particular, L2791-02 uses a lens cap that delivers even narrower directivity. As a variant type not using a microball lens, L2791-03 is also available with the LED chip potted with resin, which gives a small emission spot of ϕ160 μm.

Features

- Small emission spot
  L2791   : ϕ400 μm
  L2791-03: ϕ160 μm
- Uniform emission: L2791/-02
- Narrow directivity: L2791/-02

Applications

- Automatic control systems
- Optical switches
- Auto-focus

■ Absolute maximum ratings (Ta=25 °C)

Parameter	Symbol	Condition	Value	Unit
Forward current	I_F		80	mA
Reverse voltage	V_R		3	V
Pulse forward current	I_{FP}	Pulse width=10 μs Duty ratio=1 %	0.5	A
Operating temperature	Topr		-30 to +85	°C
Storage temperature	Tstg		-40 to +100 *	°C

* L2791-03 is guaranteed to resist temperature cycle test of up to 5 cycles.

■ Electrical and optical characteristics (Ta=25 °C)

Parameter	Symbol	Condition	L2791			L2791-02			L2791-03			Unit
			Min.	Typ.	Max.	Min.	Typ.	Max.	Min.	Typ.	Max.	
Peak emission wavelength	λp	I_F=50 mA	850	880	910	850	880	910	850	880	910	nm
Spectral half width	$\Delta\lambda$	I_F=50 mA	-	60	-	-	60	-	-	60	-	nm
Forward voltage	V_F	I_F=50 mA	-	1.5	1.7	-	1.5	1.7	-	1.5	1.7	V
Pulse forward voltage	V_{FP}	I_F=0.5 A	-	3.2	4.0	-	3.2	4.0	-	3.2	4.0	V
Reverse current	I_R	V_R=3 V	-	-	10	-	-	10	-	-	10	μA
Radiant flux	ϕe	I_F=50 mA	1.6	2.0	-	1.6	2.0	-	4.0	5.0	-	mW
Radiant illuminance	P_E	I_F=50 mA	-	1.3	-	-	2.0	-	-	-	-	mW/cm²
Rise time	tr	I_F=50 mA, 10 to 90 %	-	0.12	0.2	-	0.12	0.2	-	0.12	0.2	μs
Fall time	tf	I_F=50 mA, 90 to 10 %	-	0.12	0.2	-	0.12	0.2	-	0.12	0.2	μs

SOLID STATE DIVISION

HAMAMATSU

1

■ Emission spectrum

(Typ. Ta=25 °C, Iv=50 mA)

WAVELENGTH (nm)
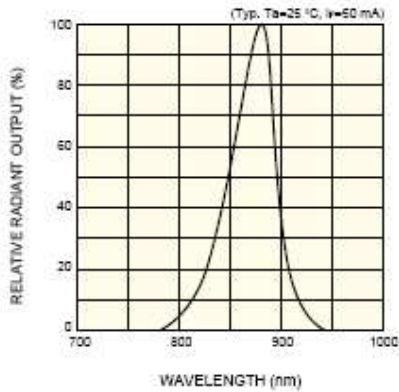
KLED291060A

■ Radiant flux vs. forward current

(Typ. Ta=25 °C, tw=100 µs, 0.1 %)
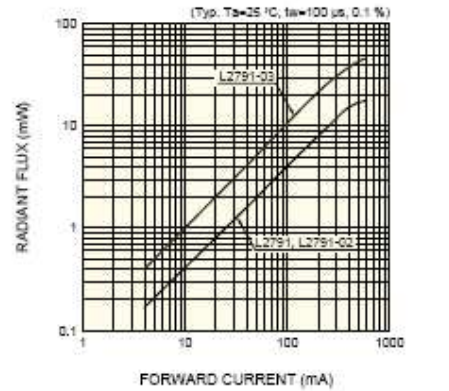
FORWARD CURRENT (mA)

KLED291040A

■ Forward current vs. forward voltage

(Typ. Ta=25 °C, tw=100 µs, 1 %)

FORWARD VOLTAGE (V)

KLED291050A

■ Directivity

(Typ. Ta=25 °C)

RELATIVE RADIANT OUTPUT (%)

* L2791-03: Except for reflection ingredient of the base.
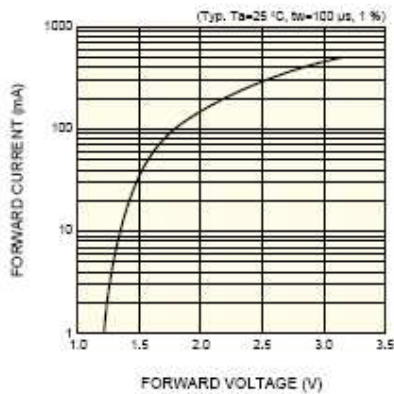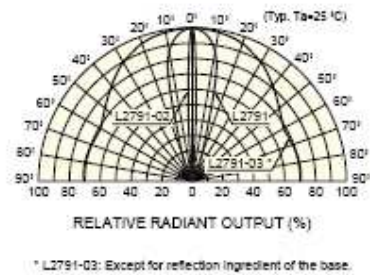
KLED291010A

■ Radiant output vs. ambient temperature

(Typ. Iv=50 mA)

AMBIENT TEMPERATURE (°C)
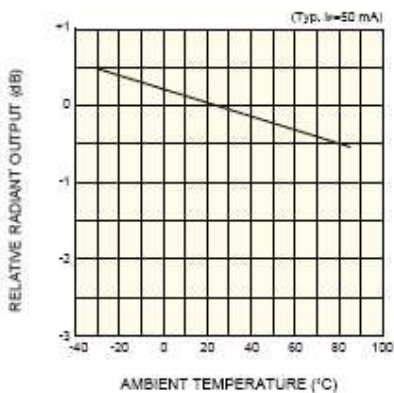
KLED291030A

■ Allowable forward current vs. ambient temperature

(Typ.)

AMBIENT TEMPERATURE (°C)

KLED291070B

2
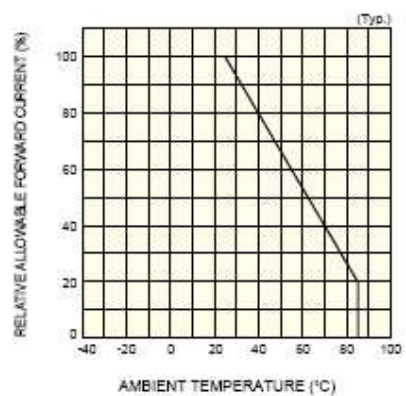
■ Allowable forward current vs. duty ratio
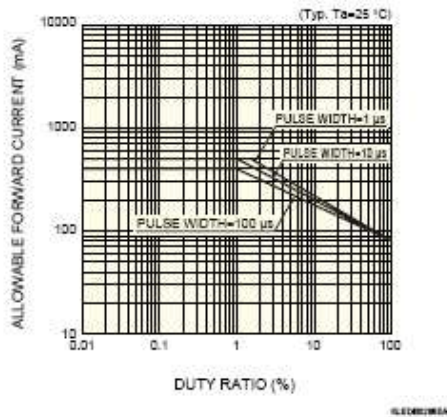
■ Dimensional outlines (unit: mm)

① L2791	② L2791-02	③ L2791-03

ACKNOWLEDGMENTS